

Rina Krautwirth

Barnard College

December 2004

BA, Biology

Advisor:

Dr. Janet Larkin

Cellular Responses to the Interaction of the Anti-  
tumor Drug Taxol with the Microtubules

© Rina Krautwirth 2003

Barnard College

December 2004

BA, Biology

Advisor:

Dr. Janet Larkin

## **Cellular Responses to the Interaction of the Anti-tumor Drug Taxol with Microtubules**

### **Abstract**

Taxol, an anti-cancer compound discovered in the rare Pacific yew tree *Taxus Brevifolia*, binds to the microtubules and stabilizes them. It effects cells primarily in G<sub>2</sub> or M phase, both of which require highly active microtubules. By interfering with the microtubules needed for the mitotic spindle, taxol alters/blocks mitosis, which decreases cell proliferation. High concentrations of taxol induce microtubule polymerization, which creates bundles in the cells. Concentrations too low to enhance polymerization still stabilize microtubule dynamics, a necessary behavior (particularly during mitosis) that involves alternating periods of rapid shrinkage, pause, and rapid growth. Increased polymerization and stabilization stems from taxol's ability to strengthen lateral interactions between the protofilaments that comprise the microtubule. The binding site for taxol on the tubulin subunit is located adjacent to a structural component termed the M-loop, which is highly involved in lateral interactions. In binding to this area, taxol decreases the flexibility of the M-loop (by changing its shape and by creating density in a previously empty area) so that lateral interactions between adjacent tubulin subunits are strengthened. The cumulative effect is to strengthen lateral connections between protofilaments, and in this way the microtubule becomes more stable. Mitotic spindles that have lost their dynamics or have accumulated into bundles will have difficulty carrying out mitosis. Unfortunately, cells have numerous ways of becoming resistant to taxol treatment.

### **Introduction**

The discovery of taxol<sup>1</sup> and its utility as a cancer drug came about in the early 1960s, when the National Cancer Institute and the US Department of Agriculture cosponsored an 'all-out scientific search' for substances in nature that could potentially exhibit anti-tumor activity.<sup>1,2</sup> In 1962, researchers found that extract from the inner bark of the Pacific yew tree, *taxus brevifolia*, did in fact inhibit tumors and five years later, Wani and Wall isolated the active compound – taxol – and identified its structure (see figure 1).<sup>3</sup>

Unfortunately, the Pacific yew tree did not turn out to be the most ideal source for a

---

<sup>1</sup> "Taxol" is trademarked by Bristol-Meyers Squibb; common name paclitaxel.

promising new medicine. The yews, which grow in protected forests in the Pacific Northwest, are not only rare but extremely slow growing, and moreover, when their bark is removed so that the medicine can be obtained, the trees die.<sup>4</sup> Furthermore, the trees yield a very small amount of taxol: taxol comprises only 0.01 to 0.03% of the dry weight of the inner bark, and a 40 foot (100 year old) tree provides 300 mg of the drug – approximately one dose.<sup>5,6,7</sup> Due to these conditions, until alternative sources of taxol were discovered, treatment remained costly. The production of a taxoid precursor baccatin III by European yew, *taxus baccata*, enabled the semi-synthesis of taxol and of the taxol-related compound taxotere (docetaxel) (see figure 1).<sup>8,9</sup> Since baccatin is produced in the needles, the source is renewable. In 1993, Stierle, Stierle and Strobel discovered that a fungal endophyte (*Taxomyces andreanae*) growing on the inner bark of the yew tree produces taxol as well, and although minute quantities resulted, microbiologists pointed out that the microbe could require an activating compound from the plant, and also that genetic engineering or increased oxygen supply could conceivably amplify the yield.<sup>10,11</sup> A monumental breakthrough occurred in 1994 with the much sought after total synthesis of taxol by two teams, one lead by Nicolaou and one by Holton, followed by Danishefsky et al in 1996 and others since.<sup>12</sup>

Upon the discovery of taxol, researchers began to investigate its mechanism of action, and identified the microtubules as its target. Originally, researchers considered the possibility that taxol worked in a manner similar to that of other known anti-microtubule compounds, namely by destabilization of the microtubules. However, a landmark paper by Schiff et al in 1979 revealed that taxol induces tubulin polymerization and in fact *stabilizes* microtubules. In the past twenty-five years since this finding, scientists have accomplished much by way of understanding how taxol interacts with the microtubules. The taxol binding site on the microtubule subunit tubulin has been located

and characterized. The structure of tubulin itself has been determined and refined, its protein sequence has been established, three domains have been assigned and nucleotide binding sites have been identified. Cellular modifications induced by taxol in terms of microtubule polymerization and dynamics, mitotic block or aberrant mitosis, centrosomal disruption and apoptosis have been characterized. Effects beyond the microtubule – pathways leading to apoptosis independent of mitotic block – have been studied.

By the time that its total synthesis had been discovered, taxol had undergone clinical trials and had received FDA approval as treatment for ovarian and breast cancers (1992 and 1994, respectively). It also acts against lung, head, and neck cancers and lymphomas, according to Rowinsky and Donehower as quoted in Abal et al (2001).<sup>13</sup> However, the problem of taxol resistance presents a challenge to its clinical effectiveness. Expectantly, further investigation yielding yet a better understanding of taxol's mechanism of action will enable this difficulty to be surmounted, bringing about an increase in the number of successful treatments.

### **Taxol: A unique molecule**

Taxol is noted for its unique structure<sup>14</sup> (see figure 1). It is a very hydrophobic molecule.<sup>15</sup> Due to the complexity of the structure, synthesis in the lab proved challenging. In terms of

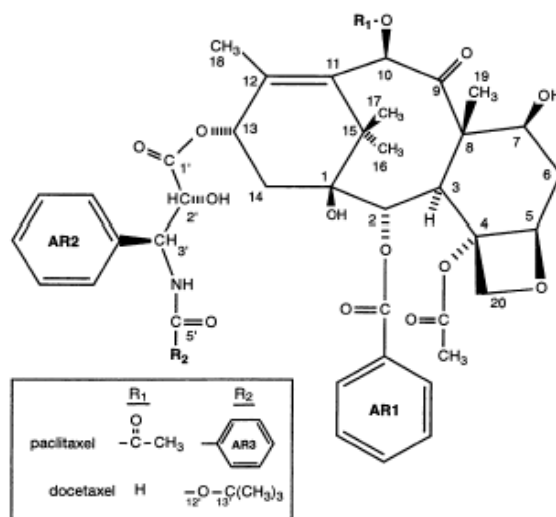


**Figure 1** Chemical structure of taxol and taxotere. Two side chains differ: at C5', taxol has a phenyl and taxotere has a tert-butyl. At C10, taxotere lacks an acyl group. (Mastropaolo, D. et al (1995). Crystal and Molecular Structure of Paclitaxil (Taxol). Proc. Natl. Acad. Sci. 92, 6920-6924.

its pharmacological effect, the structure activity relationship (SAR) dictates that the C2 bezoate is essential, as are the two side chain components of C13– C3'-N-benzoyl and C3' phenyl (see figure 1).<sup>16</sup> These areas engage in crucial hydrophobic interactions with the hydrophobic binding pocket on the monomer of the tubulin dimer (see below).<sup>17</sup> The hydroxyl group at the 2C' is also necessary.<sup>18</sup> Experiments using a fluorescent analogue (FLUTAX) that had an acetyl replacement at the 2'C had 500 times weaker activity.<sup>19</sup> In terms of the cumulative activity of the side chains, baccatin, which has only the core structure, has 1000 times less activity (see figure 2).<sup>20</sup>

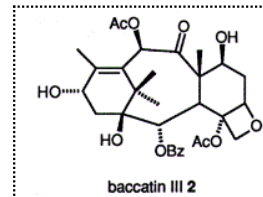


**Figure 2.** Baccatin III2 derives from the European yew tree. It is identical to the core of the taxol and taxotere molecules.

Taxotere (docetaxel) for the most part has the same structure as taxol. Differences occur at C10, where taxol's acetyl is replaced by a hydrogen, and on the C3'-N-benzoyl, where the ring is replaced by a linear conformation (see figure 1).

Photoaffinity and electron crystallography studies enabled the mapping out of structural components of taxol against corresponding sections of its binding site on the microtubule (see below). Along with characterization of the site, it was possible also to arrive at the probable conformation of bound taxol. Rotation of a carbon-to-carbon bonds shifts the spatial orientation of the side chains.<sup>21</sup> This creates the possibility for a molecule to exist in a number of different conformations, termed conformers.<sup>22</sup> Snyder et al (2001) compared various conformers of the taxol molecule to a density map of tubulin (see figure 3). The T-shaped conformation favored by their results is neither polar or non-polar, in contrast to other proposals that designated the bound conformation as either one or the other (see figure 4).<sup>23</sup> Hydrophobic collapse occurs in the other two types of conformer, so that hydrophobic areas interact within the molecule itself rather than with the

protein, but this does not occur in the arrangement associated

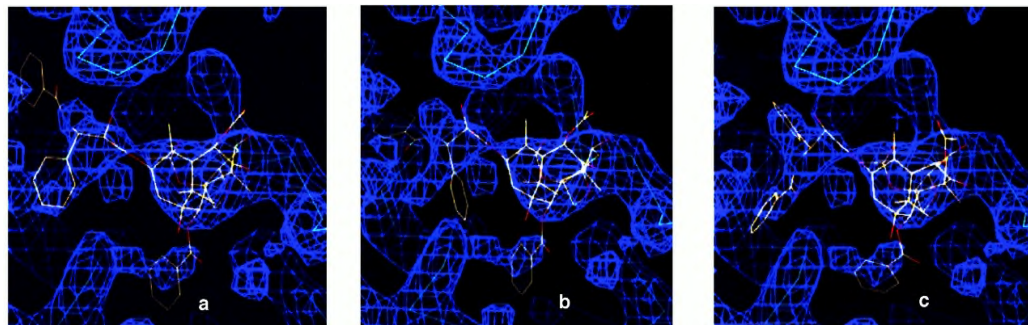


**Figure 3** Three conformers mapped against an image of the microtubule binding site. Conformer C was designated as the best fit. (Snyder 2001)

conformation, in which an amino acid of tubulin (His-229) separates the two

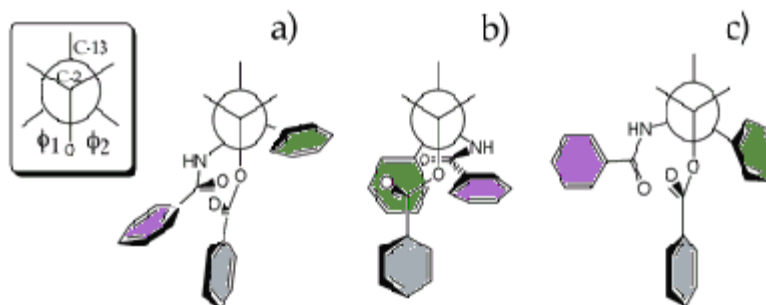


**Figure 4** The phenyl groups of taxol have many possible locations with respect to each other. Three such conformers are shown here, at C2 and C3'.<sup>24</sup> This corresponding to the images in figure 3. (Snyder 2001) [Colors added]

distinction is believed to have bearing on the synthesis of taxol-like compounds, and in fact inactivity has been found in a synthesis that induced this type of hydrophobic interaction.<sup>25</sup>

As a plant compound, taxol is classified as a diterpene. Terpenes generally fit into the category of secondary metabolites due to lack of involvement in elemental processes such as photosynthesis, respiration and nutrient assimilation.<sup>26</sup> Instead, the secondary metabolites, which in addition to terpenes include phenolic compounds and nitrogen containing compounds, serve as defense chemicals that protect against herbivory, microbial infection, etc. These substances tend to be species-specific. Terpene synthesis occurs via assembly of five carbon building blocks; diterpenes consist of two 10 carbon monoterpenes. (Plants can synthesize the five carbon structural units either through the mevalonate pathway or the methylerythritol (MEP) pathway. In the former, three

molecules of acetyl CoA from primary metabolism form the six carbon mevalonic acid, which then converts into isopentyl diphosphate (IPP), a five carbon building block. In the MEP pathway (which occurs in the chloroplast), the three carbon glycerol 3-phosphate (G3P) combines with two carbons from pyruvate to form the five carbon MEP, which becomes the five carbon structural unit dimethylallyl diphosphate).<sup>27</sup> As in the case of taxol, terpenes can form ring structures as well.

One area of exploration has been to identify biosynthetic triggers of taxol. In the fungus discovered by the Stierle team, radioactive tagging identified acetic acid and L-phenylalanine– a benzoyl source– as biosynthetic precursors of taxol (and other related compounds produced by the fungus).<sup>28</sup> In trees, leucine was identified as a precursor but not so in the endophyte.<sup>29</sup>

### **Microtubule dynamics are essential for mitosis**

Microtubules are a particularly apt target for anti-tumor drugs such as taxol because they form the mitotic spindle, which, if improperly formed, could interfere with mitosis. Significantly, the dynamic instability displayed by microtubules– alternating periods of rapid growth, pause, and rapid shrinkage– is essential for the breakdown of the cytoskeleton during late interphase, reassembly into the mitotic spindle to align chromosomes at the mitotic plate, and the mechanics of pulling each set of chromosomes to its respective pole. Taxol blocks cells primarily during the second growth stage or the mitotic stage of the cell cycle.<sup>30</sup> By binding to the microtubules, taxol can inhibit their mitotic activity and thus decrease cancer cell proliferation.

### **Tubulin is the building block of the microtubule**

Once the interaction between taxol and microtubules had become evident, it became important to better characterize tubulin, the structural subunit of the microtubule. As visualization techniques improved, the structure of tubulin could be identified and refined. Studies in 1995 were



carried out at 6.5 angstrom resolution, and by 1998 this had improved to 3.7 . In 2001, these results were further refined.

Tubulin, a self-assembling<sup>31</sup> dimer composed of  $\alpha$ -tubulin and  $\beta$ -tubulin, polymerizes to form longitudinal protofilaments, and thirteen (usually) of these protofilaments join laterally to form the hollow, cylindrical microtubule structure.<sup>32</sup> The  $\alpha$  and  $\beta$  monomers share a forty-percent sequence homology and are structurally similar, differing primarily in certain loop regions.<sup>33</sup> Whereas the nucleotide binding site of the  $\alpha$  monomer is exchangeable, that of  $\beta$ -tubulin is not.<sup>34</sup> Furthermore, only  $\beta$ -tubulin contains a taxol binding site.<sup>35</sup> A loop at the corresponding area on the  $\alpha$  monomer contains eight additional residues and blocks the area.<sup>36</sup>

Each  $\alpha$ - and  $\beta$ -tubulin protein consists of two  $\beta$ -pleated sheets— one of six sheets and one of four sheets— surrounded by twelve helices and an additional six small helices (see figure 6).<sup>37</sup> It contains approximately 450 residues and is divided into three domains: the N terminal (1-205; secondary structures S1-S6, H1-

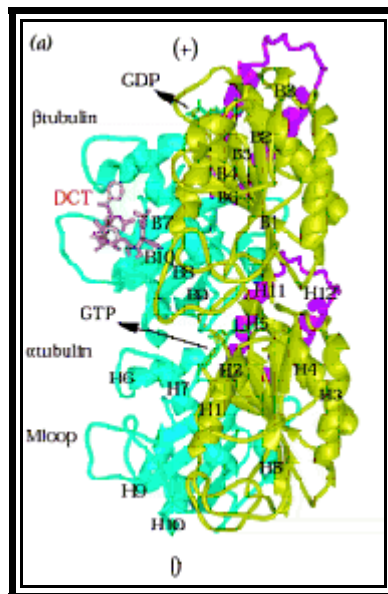


**Figure 5** Ribbon diagram of tubulin with taxotere (DCT) bound to it. N-terminal (nucleotide binding): yellow. Intermediate domain (taxol binding): blue. C terminal (binds MAPs and motor proteins): pink helices. Arrows indicate nucleotide binding sites. (Keskin 2002).

H5) contains a nucleotide binding site, the intermediate domain (206-381/S7-S10, H6-H10) contains the taxol binding site and the C terminal (382-440/H11-H12) interacts with microtubule associated proteins (MAPs) and motor proteins (see figure 5).<sup>38,39</sup> In the N terminal, loops T1 through T6 link

the alternating sheets and helices in a pattern consistent with the Rossman fold that is characteristic

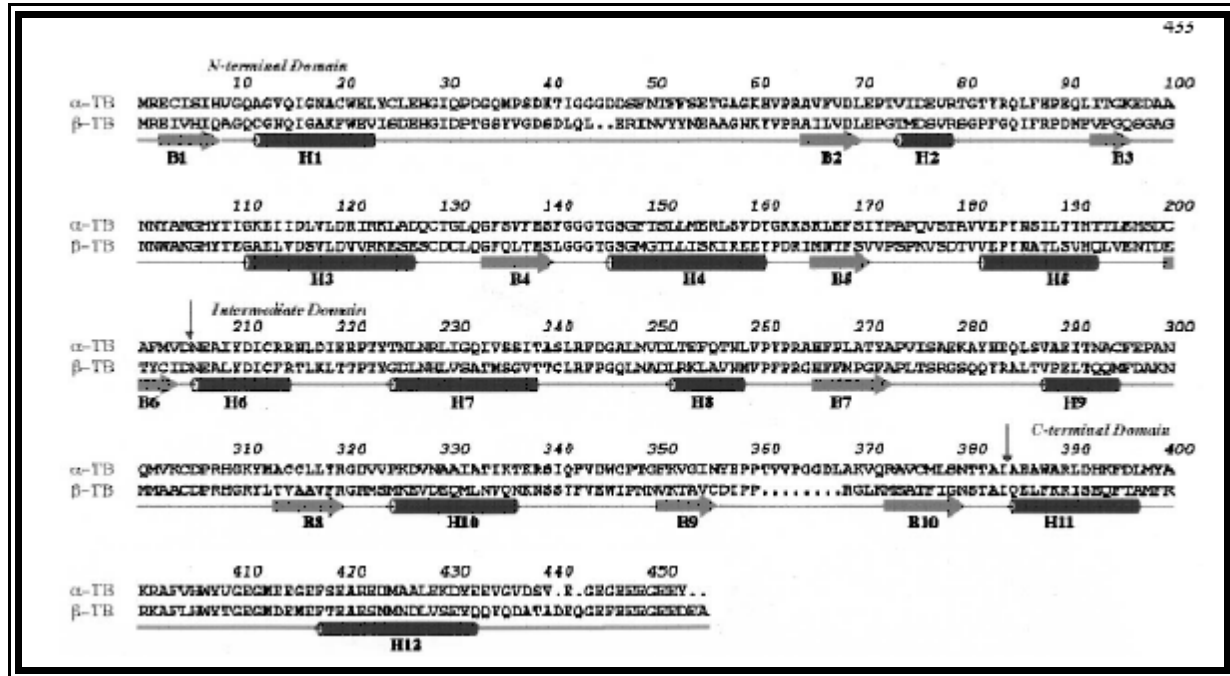


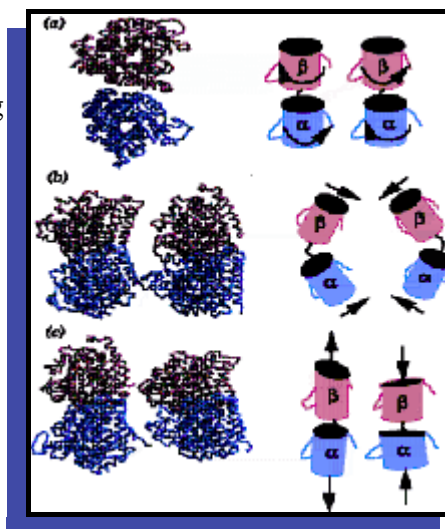
**Figure 6** Protein sequence of  $\alpha$ - and  $\beta$ -tubulin (upper and lower rows, respectively). Secondary structures are indicated (H- helix, B- sheet) and domains are marked off. (Downing 1998).

of nucleotide binding sites.<sup>40</sup> The two helices of the C terminal (H11 and H12) wrap around the tubulin molecule, and in one model, face the outside of the microtubule as well.<sup>41</sup> Some flexibility exists within this domain designation, as taxol interacts with the N terminal and the nucleotide has contact with the intermediate area.<sup>42</sup>

In terms of mobility, the tubulin unit as a whole exhibits predominantly three types of motions: torsion and wobbling that occur between the two monomers and longitudinal stretching overall (figure 7).<sup>43</sup> Within the dimer, Keskin et al have mapped out six regions that have varying levels of mobility.<sup>44</sup> Loops “involved in recognition of adjacent regions” exhibit the most flexibility

whereas nucleotide binding sites display the least amount of mobility<sup>ii</sup>.<sup>45</sup> The M-loop (a loop that

**Figure 7** Tubulin subunits have three dominant motions: a) torsional b) wobbling c) stretching (Keskin 2002).



links S7 and S9), which is involved in lateral interaction between protofilaments of the microtubule, shows high levels of flexibility at residues 280-285.<sup>46</sup> In response to taxol, the M-loop on  $\alpha$ -tubulin becomes more rigid and this could account for the increased microtubule stability that taxol induces.<sup>47</sup>

**On tubulin, the taxol binding site is strategically located for enhancement of microtubule stability**

Initial photoaffinity labeling with tritium and subsequent electron crystallography techniques allowed for the identification of the taxol binding site on the  $\alpha$  unit of the tubulin dimer. Through photoaffinity studies using tritium labeled taxol analogues, binding targets of the C3', C2 and C7 side chains were located. [<sup>3</sup>H]3'-(p-azidobenzamido)taxol indicated the affiliation of the C3'-N-benzoyl

---

<sup>ii</sup> This is in keeping with function: as a trend, areas of high mobility are involved in recognition whereas areas of low mobility are associated with binding sites such as nucleotide or catalytic sites.

with residues 1-31 of the N terminus, [<sup>3</sup>H]2-(m-azidobenzoyl)taxol showed the proximity of the C2 phenyl to a second site at 217-231, and [<sup>3</sup>H]7-(benzoyldihydrocinnamoyl)taxol (see figure 8) found Arg282, located in the M-loop, as a site of photo-incorporation of the C7 side chain.<sup>48</sup> Results of electron crystallography upheld these findings, to a close extent, finding that the C3' group binds near 15-25 and the C2 side chain binds near 212-222.<sup>49</sup>

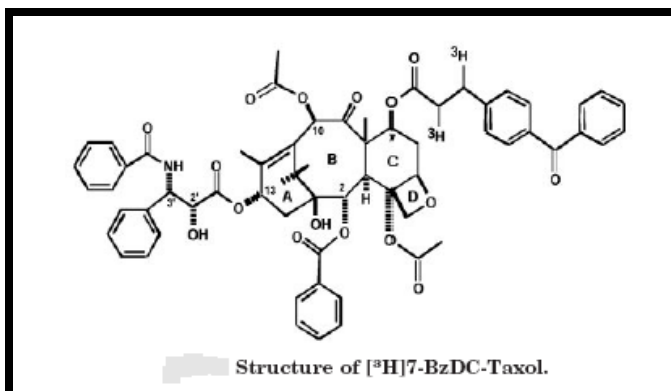


**Figure 8**

Refinement of this model provided more specifics about the site location. The secondary structures that interact with taxol are: helices H1, H6, H7 and loop H6-7, the M loop (joining S7 and S9), loop S9-S10, and sheets S8 and S10 (see figure 9).<sup>Ref.50</sup> In H1, Val23 has an isopropyl group connecting to taxol's C3'-benzamido group, and Lys19 and Glu22 have methylene groups contacting this same section of taxol.<sup>51</sup> Asp26 can hydrogen bond with the nitrogen group of C3'.<sup>Ref.52</sup> In the H6-H7 loop, Leu217 and Leu219 contact the 2-phenyl of taxol.<sup>53</sup> At H7, Asp226 (its methylene), His229<sup>Ref.54</sup> and Leu230<sup>Ref.55</sup> interact with the 2-phenyl. Ala233 and Ser236 connect to the 3'-phenyl<sup>56</sup> and Ala233 additionally, along with Leu230, interacts with the C4 acetate.<sup>57</sup> The M-loop is in the vicinity of the oxane ring that is part of the taxol molecule's main structure.<sup>58</sup> In the M-loop, Phe272 (which adjoins the 3'-phenyl as well),<sup>59</sup> Pro274, the methyl of Thr276, Leu286 and Leu291 are in juxtaposition with the C4 acetate,<sup>60</sup> Leu275, Ser277, and Arg278 connect with other areas of taxol's oxane ring,<sup>61</sup> and Thre276 has an additional connection to the C8 methyl, which is also meet with Gln281.<sup>Ref.62</sup> In the S9-S10 loop, Pro360, Leu371, and the methylene of Ser374 adjoin

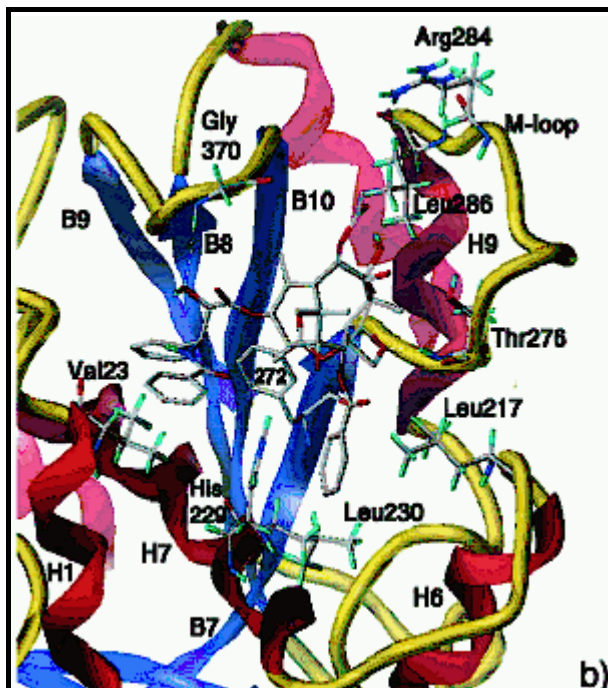


**Figure 9** Ribbon diagram of taxol binding site on  $\beta$ -tubulin. Secondary structures and some sequences are shown. M-loop links B7 sheet to H9 helix. H1 (Val 23): 3'-N-phenyl of taxol; H7 (His229): 2-phenyl of taxol. M-loop (Thr276, Arg 284): C4 acetate. (Snyder 2001).

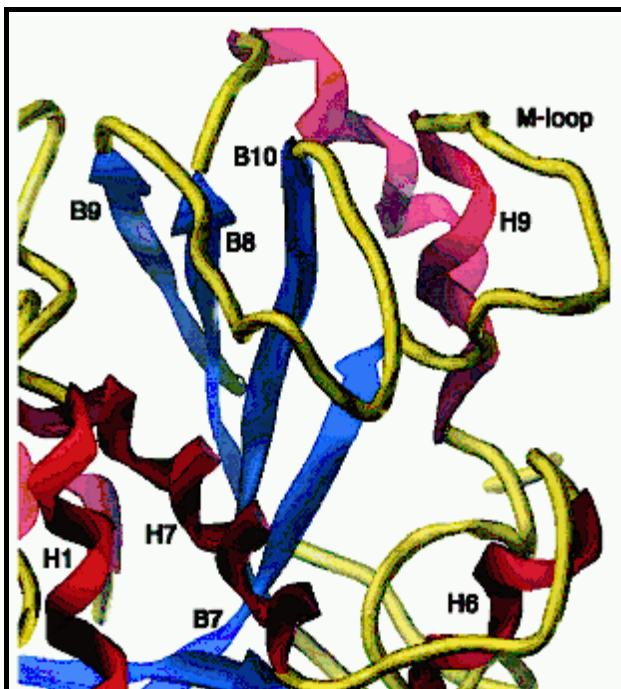


**Figure 10** Area on  $\beta$ -tubulin corresponding to the taxol binding site. The S9-S10 (here, B9-B10) loop contains eight additional residues and its length obscures the binding area. This loop also may stabilize the M-loop. (Snyder 2001).

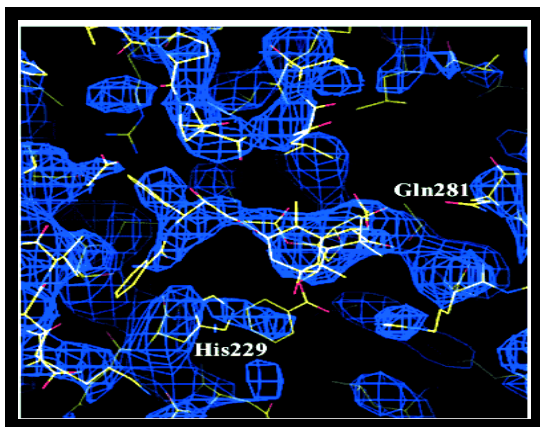


**Figure 11** Taxol structure(white) mapped against density image of tubulin (blue). His229 separates two of the phenyl rings from interacting. (Snyder 2001).

the C4 acetate, while Leu371 has an additional connection to the C12 methyl. In the Snyder model, His229 is significant for its separation of 2-phenyl from 3'-phenyl, preventing their interaction<sup>63</sup> (see figure 11).

The binding pocket for taxol on  $\beta$ -tubulin is hydrophobic and therefore there are hydrophobic interactions between the hydrophobic taxol molecule

and the binding area.<sup>64</sup> Snyder et al suggest that taxol, upon binding, converts a formerly hydrophobic area to one that is hydrophilic.<sup>65</sup> The conferral of hydrophilicity upon a previously hydrophobic area would alter the nature of the tubulin dimer, which would somehow have implications for the lateral interactions and their ultimate impact on the overall microtubule in terms of polymerization and stability.<sup>66</sup> Moreover, with the addition of taxol, the altered binding pocket would then gain similarity to the corresponding area on the  $\beta$ -unit, where the S9-S10 loop has eight additional residues— Thr361 to Leu368— and blocks the site from being open (see figure 10).<sup>67</sup> This S9-S10 loop conformationally stabilizes the M-loop on  $\beta$ -tubulin.<sup>68</sup> As such, the taxol molecule would perform a function in  $\beta$ -tubulin analogous to that of the longer S9-S10 loop in the monomer.<sup>69</sup> In addition, the M-loop itself “includes a segment of the sequence that is one of the most divergent between  $\alpha$ - and  $\beta$ -tubulin.”<sup>70</sup>

Taxol effects tubulin mobility in a number of areas. In the  $\beta$  unit, it decreases flexibility not only at 272-285 within the M-loop but at 35-44, 214-224, and 351-378, in loops located in the area surrounding the taxol site.<sup>71</sup> In terms of the M-loop, upon taxol binding, the “increase in packing density” in the formerly empty site could be responsible for the resultant increase rigidity.<sup>72</sup> Moreover, the binding of the molecule could cause a change in shape of the M-loop that would likewise decrease its flexibility.<sup>73</sup> By causing the M-loop to become less flexible, taxol strengthens lateral interaction between protofilaments, thereby increasing the stability of the microtubule as a whole.<sup>74</sup>

At the C-terminal domain of  $\beta$ -tubulin, in contrast, mobility increases.<sup>75</sup>

Taxol also alters the mobility of  $\alpha$ -tubulin, but in this monomer, in contrast to its impact on  $\beta$ -tubulin, taxol induces an increase in flexibility.<sup>76</sup> The M-loop (at 276-286) in fact becomes more



flexible.<sup>77</sup> Additionally, increased flexibility was observed at residues 32-62 of the N terminal and 439-440 of the C terminal.<sup>78</sup> As such, taxol somewhat reverses the mobility of each monomer. The functional significance of the increased mobility at the C-terminal and of the monomer was not delineated.

**Lateral and longitudinal contacts stabilize the microtubule structure**

Longitudinal polymerization between dimers creates thin protofilaments (see figure 12). However, a structural system consisting of such thin protofilaments would likely be unstable.<sup>79</sup>

Instead, the protofilaments form lateral connections as well, which strengthens the structure.<sup>80</sup> However, there still remains some flexibility at the ends of the polymer because there the subunits have the ability to dissociate.<sup>81</sup>

Microtubules have a 25 nm total diameter<sup>82</sup> with a 16 nm inner diameter.<sup>83</sup> Lengthwise, tubulin dimers repeat at 8 nm intervals.<sup>84</sup> The protofilaments created by the longitudinal attachment

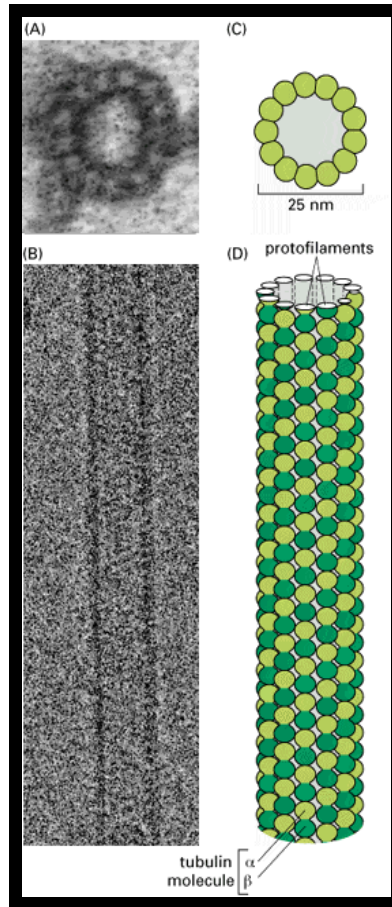


**Figure 12** Tubulin units assemble into thin protofilaments that arrange into a hollow tube with a 25nm diameter. A, B: electron micrograph. (Alberts 3<sup>rd</sup> Edition).

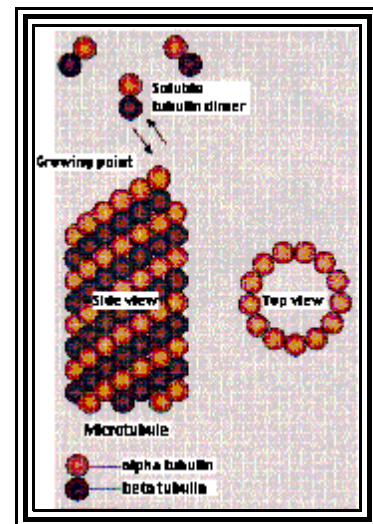


**Figure 13** Close-up of microtubule. Protofilaments align in a parallel fashion. However, slight offset creates helical surface pattern.

of tubulin dimers form a parallel alignment, with monomers laterally adjacent to each other and monomers laterally adjacent to each other<sup>85</sup> (see figure 13). However, these lateral connections occur on a slant (~9 nm offset), so that the rows create a helical pattern wrapping around the microtubule surface<sup>86</sup> (see figure 13). The way in which the subunits bind to each other creates small (1-2 nm) gaps, or fenestrations, on the surface of the microtubule.<sup>87</sup> Whether or not taxol would be able to diffuse through these gaps to reach an internal binding site has been debated.

The parallel alignment creates structural polarity, with a row of units at the designated plus end and a row of .at the minus end.<sup>88</sup> There is also functional polarity. Because at the plus end the upper surface of the units, with exposed GTP, face the growing end whereas at the minus end, the lower surface of the monomers, lacking exposed GTP, face the growing end, the plus end becomes more dynamic.<sup>89</sup> In animal cells, the minus end is anchored in the microtubule organizing center (centrosomes) while the plus end extends toward the periphery of the cell.<sup>90</sup> In mitotic cells, the minus ends remains at the centrosomes while the plus ends attach to the kinetochores.<sup>91</sup>

The secondary structure areas of the tubulin monomer involved in longitudinal contact are: the H10-S9 loop with H11 and loop T5 of the monomer below and H10 with H6 and the H6-H7 loop above; H8 with part of loop T5, loop T3, and the H11 to H12 loop below; loop T7 with loop T1, H2 and H7 in the monomer above and with the nucleotide above it as well.<sup>92</sup>

The structurally analogous areas of and tubulin involved in contact within the dimer (intradimer) and between dimers (interdimer) (lower and upper ends of each) contain differences in amino acid residues.<sup>93</sup> This becomes significant in that the exchange of some hydrophobic residues at the meeting point within the dimer for hydrophilic replacements in the contact area between dimers plays a role in monomer stability as compared to dimer stability.<sup>94</sup> For example, two of the



amino acids present in the intradimer area create a stabilizing “salt bridge” that is absent from the interdimer area: the positively charged arginine ( 253) interacts with the negatively charged aspartic acid ( 98) whereas at the interdimer area, these residues are replaced by ones that are uncharged polar and non-polar, respectively.<sup>95</sup> In this way, intradimer connections have more stability than those between two dimers.<sup>96</sup> Observation of decreased flexibility in residues involved in intradimer contact supports this model. Residues 172-181, located at the top of each monomer, are less flexible in  $\beta$ -tubulin than they are in  $\alpha$ -tubulin.<sup>97</sup>

Because the determination of tubulin structure derived from microtubules assembled on zinc sheets, and microtubules formed in this way align in an anti-parallel rather than the usual parallel manner, this system could not provide information about areas involved in lateral contact.<sup>98</sup> As a

solution to this, Nogales et al superimposed (“docked”) the 3.7 Å tubulin model onto a lower resolution “3D map” of the microtubule, so that if placed correctly, fitting the detailed image of tubulin onto the microtubule would give a detailed image of the microtubule (see figure 14).<sup>99</sup> A later study made use of the same technique with a higher resolution (14 Å) map of the microtubule.<sup>100</sup>

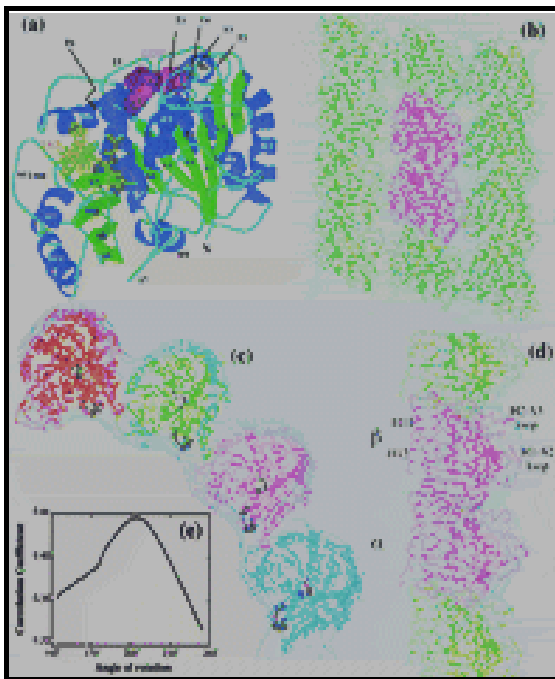


**Figure 14** Docking of high resolution tubulin model into lower resolution microtubule model. A) tubulin B, C, D) front view from outside microtubule, cross section, lateral view. [E) graph relating to fit.] (Nogales 1999a).

Aside from the M-loop, areas involved in lateral contact include loop H10-S9 with H4 of

the adjacent monomer and loop H6-H7 with H3 of the adjacent monomer<sup>101</sup> (see figure 15). In terms of lateral assembly, Keskin et al suggest that and undergo “rigid body rotation” in opposite

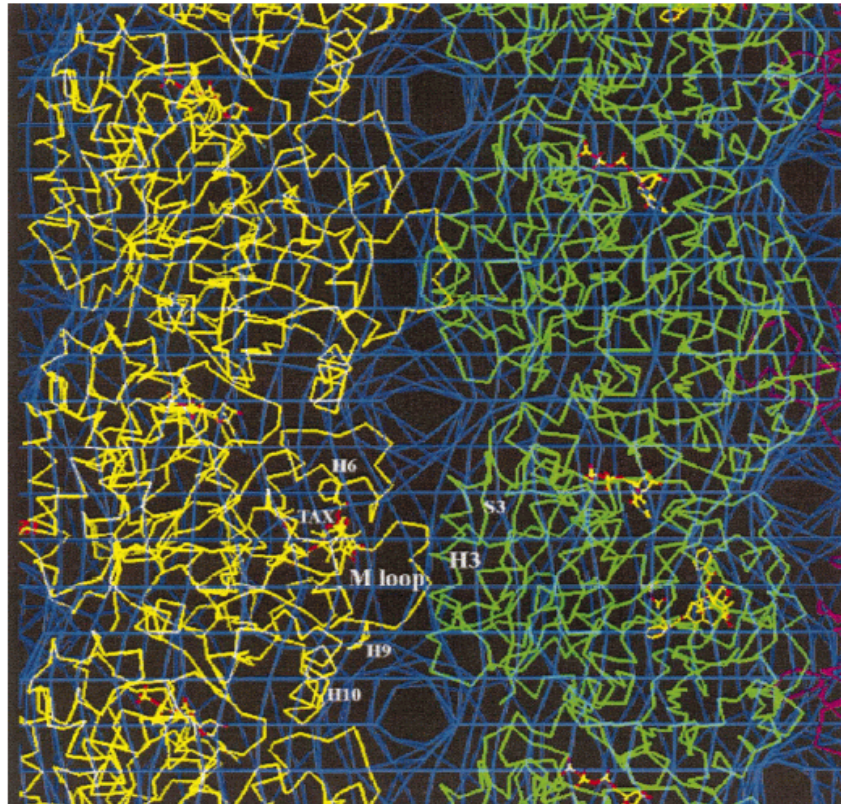


**Figure 15** Docking of protofilament structure onto 2D map of the microtubule (blue). Lateral contacts of two adjacent protofilaments are marked off: M-loop, H6, H9, H10 (yellow); H3, S3 (green); taxol (TAX) bound near M-loop. (Nogales 1999b).

directions from each other, toward the interprotofilament area on either side<sup>102</sup> This motion seems to turn adjacent monomers in toward each other while the monomers on those same protofilaments turn outward toward monomers on opposite sides. The stretch motion (shown in figure 7c) may also contribute to lateral interactions, because it causes the M-loop to shift outward.<sup>103</sup>

According to the high resolution microtubule model, helices H11 and H12 of the tubulin units face the outer surface of the microtubule, as does the H10-S9 loop.<sup>104</sup> The inner surface is more bumpy, containing loops (H1-S2 loop and H2-S3 loop, S9-S10 loop) [see figure 16].<sup>105</sup>

Normally, 13 protofilaments arrange to form the microtubule, although variations do exist amongst different species– the microtubules of *C. elegans*, for example, have only eleven protofilaments (with the exception of certain sensory cells that have 15).<sup>106</sup> In the cell, the centrosomes establish the number of protofilaments.<sup>107</sup> However, *in vitro*, various factors can alter this number. Taxol-induced microtubules, for example, only contain 12 protofilaments.<sup>108</sup> One explanation offered is that the presence of taxol decreases the bond angle between protofilaments (from 152.3° to 150°), narrowing the circle and allowing for one less protofilament.<sup>109</sup>

Complete parallel alignment only occurs in a microtubule with an even number of protofilaments.<sup>110</sup> In a structure with an odd number, the odd protofilament aligns in an antiparallel fashion, which creates what is termed a “seam.”<sup>111</sup> This seam is thought to have a destabilizing effect, presumably because of the difference between a lateral connection of an  $\alpha$  monomer with a  $\beta$  monomer and a connection between two monomers of the same type.<sup>112</sup> Sequential differences on both lateral surfaces of each monomer account for the stronger connection between two identical monomers.<sup>113</sup>

### **Orientation of taxol binding site on the microtubule is disputed**

Although the location of the taxol binding site with respect to tubulin has been established, there has been some dispute as to where the site is placed on the assembled microtubule. Initial findings showed that the lumen of the microtubule contains the site. The 3.7 Å tubulin model that was “docked” into a density map of the microtubules to provide a high resolution model of the

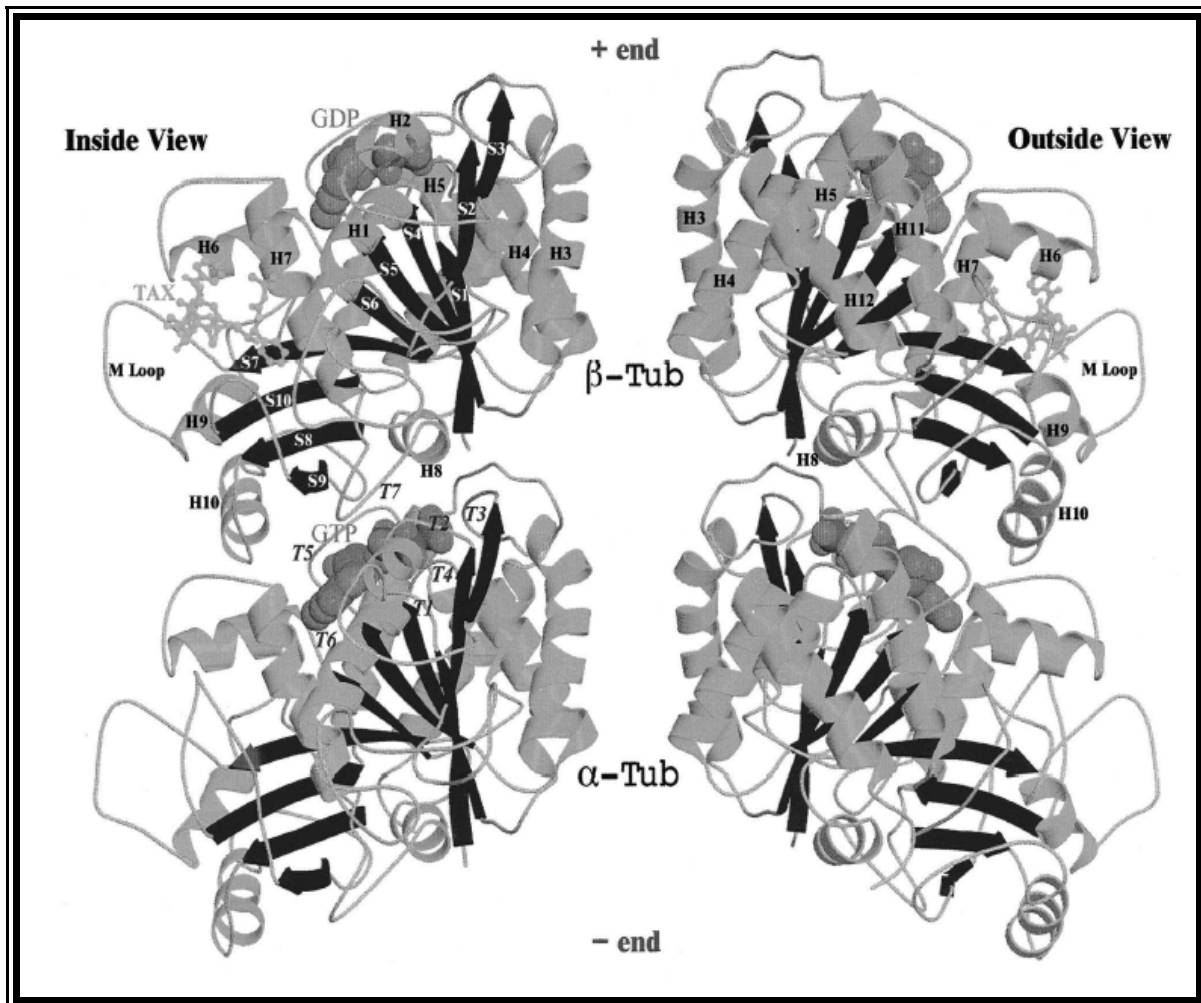


**Figure 16**

Tubulin structure as viewed from inside and outside of the microtubule. Loops T1-T7 are at the inner surface. C-terminal helices H11 and H12, which interact with MAPs and motor proteins, are outside. (Nogales 1999b).

microtubule placed the taxol site in the lumen.<sup>114</sup> However, the results of kinetic studies suggested that taxol binds too quickly to allow for an internal site; instead, there must be easy access.<sup>115</sup> Kinetics rule out the possibility that taxol diffuses in through microtubule ends, and size and probability considerations seem to exclude the possibility that taxol diffuses through “fenestrations”

in the microtubule wall.<sup>116</sup> In response, Diaz et al raise the possibility of a rotated model— turning the protofilaments 30° on the high resolution model would keep the site where it is on the dimer but would reposition it into the interprotofilament area. There is flexibility within the docking for this adjustment; however, certain conflicts with prior observations regarding location of residues still need adjustment (for example, conflicts with assigned placement of loops on the inner or outer surface of the microtubule).<sup>117</sup> An earlier study also maintains that the taxol binding site is located in the gaps in between protofilaments.<sup>118</sup> In this way, the molecule decreases the bond angle between the individual protofilaments, an explanation offered for why taxol decreases the number to 12. <sup>Ref.</sup><sup>119</sup> In their study on taxol mobility through the microtubule, Ross et al utilized the model that places the site in the lumen, and maintain that the surface fenestrations are in fact large enough to accommodate the ~1nm taxol molecule.<sup>120</sup> Providing a possible solution, Li et al recently were able to obtain an 8 Å resolution image of microtubule, “intact” rather than formed on zinc sheets, which provided enough detail for visualization of secondary structures, including the M-loop (Li, 2002). This revealed certain differences between microtubules formed on zinc sheets and those with regular alignment, with implications for taxol binding (Li, 2002). Specifically, in microtubules formed on zinc sheets, the M-loop contacts H6 of its own monomer but in regular microtubules this contact seems to break, resulting in a more mobile H6 and the M-loop “shifted downward” (Li, 2002). This would create gaps that would certainly be large enough to accommodate taxol, enabling it to reach the interior quickly (Li, 2002). Taxol in fact does occupy space between the M-loop and H6 (see figures 5 and 16). (The kinetic study (Diaz 2000) does not mention zinc sheets).

## **GTP**

The hydrolysis of guanosine-triphosphate to guanosine-diphosphate often provides energy for reactions and can serve as a regulator between the active and inactive forms of a molecule. Examples of nucleotide binding proteins include Ran, which regulates transport between the nucleus and the cytoskeleton,<sup>121</sup> and elongation factors, which control the translational stage of protein synthesis.<sup>122</sup> Similarly, the  $\beta$  unit of the tubulin dimer can alternate between GTP and GDP bound states. Upon polymerization, GTP hydrolysis results.<sup>123</sup> Indicative of the increased polymerization due to taxol, Hamel et al observed that an increase in GTP hydrolysis accompanied taxol-induced tubulin polymerization in a 1:1 relationship.<sup>124</sup>

As mentioned, the nucleotide binding site is located in the N terminal domain. The “signature motif” of tubulin (glycine rich– GGGTGSG) is located within the GTP binding domain<sup>125</sup> and interacts with the nucleotide.<sup>126</sup> In keeping with its catalytic function, the nucleotide binding area has low mobility.<sup>127</sup>

The nucleotide binding site of the  $\alpha$  monomer, the N-site, is non-exchangeable whereas that of  $\beta$ -tubulin, the E-site, allows for exchangeability. Their structural positions account for this: since the nucleotide binding site is located at the upper end of each monomer, situation of the  $\beta$ -tubulin unit beneath the  $\alpha$  monomer obscures its nucleotide binding site, while the site on the  $\beta$  subunit remains openly accessible until another dimer adds on.<sup>128</sup> Upon polymerization, because the monomer has now become obscured by the unit above it, its nucleotide site likewise becomes non-exchangeable. After polymerization, the lower end of the  $\beta$ -tubulin of the incoming dimer serves as a catalytic site causing GTP hydrolysis at the E site.<sup>129</sup> For example, within a polymerized

microtubule, the nucleotide in the E site of  $\beta$ -tubulin contacts residue 254 of  $\alpha$ , glutamic acid, which assists in GTP hydrolysis.<sup>130</sup> This is in contrast to within the monomer, in which GTP at the N site of  $\beta$ -tubulin instead contacts lysine at residue 254 of  $\alpha$ -tubulin, and this interaction has a stabilizing effect.<sup>131</sup> As such, the difference in the type of amino acids at structurally analogous areas of  $\alpha$  and  $\beta$  tubulin (hydrophobic replacements at the intradimer interface for hydrophilic residues in the interdimer area) that plays a role in monomer stability as compared to dimer stability includes effects on interactions with the nucleotide binding site (see figure 17).<sup>132</sup>

The hydrolysis at the E site upon polymerization has a number of ramifications on overall microtubule behavior, in terms of both polymerization and steady state dynamics. Replacement of GTP with GMPCPP, which hydrolyzes at a much slower rate, creates more stable microtubules, indicating that disassembly does not occur in the absence of hydrolysis.<sup>133</sup>

The fundamental cause of microtubule dynamics is the fact that relative to the GTP bound

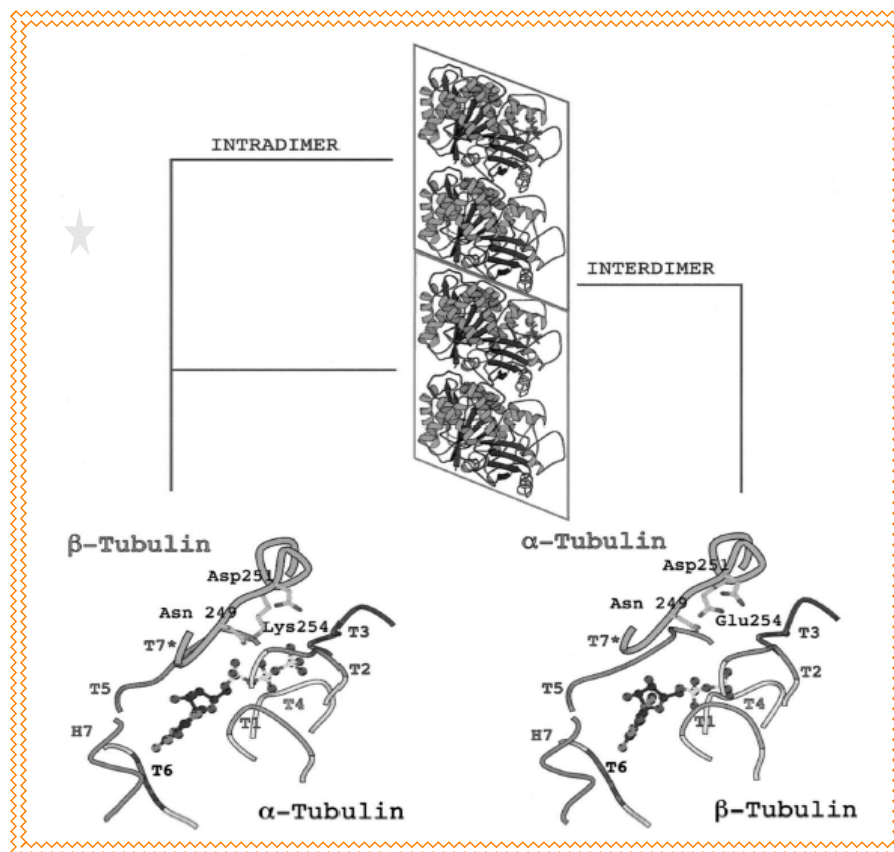


**Figure 17** Comparison of longitudinal contact within the dimer and between dimers. At 254,  $\beta$ -tubulin contains a lysine, which stabilizes the contact, whereas  $\alpha$ -tubulin contains glutamic acid, which assists in nucleotide hydrolysis. (Nogales 1999b).

form, GDP tubulin has a higher rate of dissociation from the microtubule.<sup>134</sup> This can be accounted



for by thermodynamic considerations. Because GTP hydrolysis releases energy into the surrounding structure and more free energy is then released following dissociation of GDP tubulin as compared to GTP tubulin, GDP tubulin has a lower affinity for the polymer.<sup>135</sup>

Structural considerations are also involved. In many cases, GTP hydrolysis causes a conformational change that accounts for the difference in activity between the two forms.<sup>136</sup> Such is the case with tubulin, in which hydrolysis to GDP causes the dimer to change shape, forming a curved configuration.<sup>137</sup> This gives it a less grounded attachment to the microtubule, so that the protofilament will “peel off and curl” (see figure 18).<sup>138</sup> Taxol-induced microtubules contain the straight rather than the curved conformation.<sup>139</sup>

The status of the nucleotide (D or T) might in fact have some bearing on lateral interactions within the microtubule, even though the nucleotide itself is located in the area of longitudinal connection.<sup>140</sup> Loop T3 in the nucleotide binding domain interacts with the third phosphate of GTP, the  $\gamma$ -phosphate, which is removed upon hydrolysis, and this same loop also interacts with helix H3,

which laterally contacts the adjacent M-loop.<sup>141</sup> Therefore, the loss of this third phosphate could conceivably alter/destabilize lateral connections. Experiments with tubulin and the destabilizer stathmin showed that as curved tubulin pulls away, it seems to pull “directly on the M-loop contact in the neighboring protofilament.”<sup>142</sup> Thus, the effect of taxol on the M-loop would prevent dissociation that normally occurs in response to conformational change created by nucleotide hydrolysis.

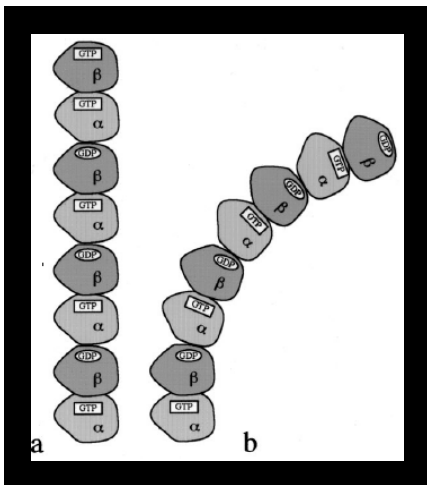


**Figure 18** A) Protofilament containing GTP tubulin. B) Protofilament containing GDP tubulin acquires curved shape. (Downing 1998).

Given the higher dissociation rate of GDP tubulin, the hydrolysis that occurs after polymerization gives the dimers a higher tendency to break off. The majority of tubulin subunits on the microtubule in fact are GDP bound.

Under these conditions, the formation of microtubules might seem unlikely. However, a GTP cap adds on to the plus end and stabilizes the growing polymer. The cap forms when dimers add on at a rate faster than that at which GTP hydrolyzes, leading to an accumulation of GTP tubulin that slows depolymerization, given that “microtubules depolymerize about 100 times faster from an end containing GDP tubulin than from one containing GTP tubulin.”<sup>143</sup> Further, the incoming dimer serves a catalytic function for hydrolysis,

but in the meantime its own nucleotide remains a Dtriphosphate; this favors the formation of a stabilizing layer.<sup>144</sup> This cap, however, remains in flux due to three possible occurrences: GTP in the cap hydrolyzes prior to addition of new units, GDP tubulin rather than the GTP bound form adds on to the polymer, or the GTP dimers in the cap in fact dissociate for some reason.<sup>145</sup> The later two remain possible because, although the tri- and diphosphate forms tend toward their respective affinity levels, it is still possible

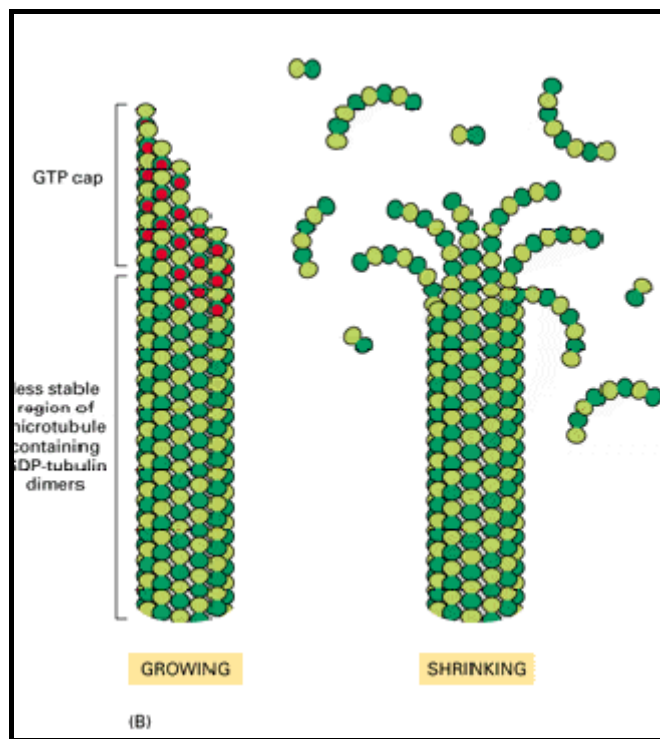


**Figure 19** If GTP tubulin units bind the microtubule plus end at a faster rate than that at which hydrolysis occurs, a stabilizing GTP cap will form. However, upon hydrolysis this cap disappears, and the GDP tubulin units in their curved conformation (see figure 18) dissociate, creating the shrinkage characteristic of dynamic instability. (Alberts 3<sup>rd</sup> Edition).

for the opposite to occur.<sup>iii</sup> The flexibility of the GTP cap creates a phenomenon termed “dynamic behavior” (see next section).

The GTP cap forms at the plus end but usually not at the minus end. Since, as mentioned, the minus end is less dynamic, its slower polymerization rate allows enough time for hydrolysis to occur before the next dimer comes along. Polar ends- plus is more dynamic, because conformational change not required. However, though the minus end consists of GDP tubulin, the centrosomes prevent it from depolymerizing.<sup>146</sup>

Upon dissociation of GDP from its microtubule, the exchangeability of its nucleotide allows it to once again acquire GTP. This increases the amount of available GTP tubulin, with its higher affinity for the polymer, promoting microtubule formation. Due to the importance of GTP in polymerization, exogenous GTP is required to generate microtubules *in vitro*. Taxol in some conditions alters the need for GTP. Through stabilization of the microtubule structure, taxol prevents dimers of lower affinity from depolymerizing, which decreases need for GTP tubulin.<sup>147</sup>

### **Behind the Dynamics: GTP Hydrolysis**

The higher dissociation rate of GDP and the hydrolysis of GTP tubulin upon polymerization creates two types of dynamic behavior: treadmilling and dynamic instability. Treadmilling occurs when polymerization and depolymerization take place at the same rate on opposite ends of the microtubule, so that the length remains constant.<sup>148</sup> Since GDP tubulin has a higher dissociation rate, it also has a higher critical concentration– the concentration of free tubulin that would favor polymerization over depolymerization– than that of GTP tubulin.<sup>149</sup> A situation can occur in which

---

<sup>iii</sup> Since more of the free tubulin is GTP bound, coupled with the fact that GDP tubulin more readily dissociates, the GTP form typically joins the polymer whereas GDP dimers leave.

the tubulin concentration is higher than the critical concentration for GTP bound tubulin, so that the plus end with its GTP cap is adding units, while at the same time, the concentration is lower than the critical concentration required by GDP bound tubulin, so that units at the GDP-containing minus end are dissociating.<sup>150</sup> The flux of units adding on to one end and leaving the other creates a treadmill effect. “Although treadmilling was initially thought as being relevant only as an *in vitro* property, recent results have shown its importance in the cell.”<sup>151</sup> Dynamic instability occurs when, at this same tubulin concentration, polymerization rate becomes faster than GTP hydrolysis, so that a stable GTP cap forms and allows for rapid growth. Then, the GTP hydrolyzes to GDP and since GDP more readily dissociates, rapid shrinking occurs. A cycle of intermittent growth and shrinkage can ensue (the switch from growth to shrinkage is called catastrophe and from shrinkage to growth is termed rescue). In the cell, this occurs at only at the microtubule plus end, because the minus end is anchored by centrosomes.

Taxol, by stabilizing contacts between tubulin dimers, decreases the amount of dynamic behavior exhibited by the microtubules.

### **Microtubule-associated proteins regulate microtubule stability**

Under normal conditions, microtubules require microtubule-associated proteins (MAPs) for polymerization.<sup>152</sup> Likewise, *in vitro* and *in vivo* experiments have shown that MAPs stabilize dynamic behavior as well.<sup>153</sup> Of the various types of MAPs, MAP4 is located in all cells<sup>154</sup> (MAP1A, 1B, 2A, 2B, 2C, tau and big tau are located in neurons;<sup>155</sup> faulty regulation of tau has been implicated in Alzheimer disease<sup>156</sup>). MAPs contain a microtubule binding domain and a region that projects from the microtubule structure.<sup>157</sup> On the microtubule, their binding region binds to the C terminal domain of tubulin,<sup>158</sup> i.e. H11 and H12, which wrap around each tubulin monomer and face the

outside of the microtubule. The positively charged amino acids of the MAP binding domain interact with negatively charged amino acids at the tubulin C terminal<sup>iv</sup>.<sup>159</sup>

The extent to which MAPs stabilize the microtubules depends upon their status in terms of phosphorylation, which inhibits them.<sup>160</sup> The highly dynamic behavior required of microtubule during mitosis results in a “sevenfold-higher degree of phosphorylation.”<sup>161</sup> Drewes et al located microtubule-affinity-regulating kinases (MARKs) that carry out this phosphorylation.<sup>162</sup>

Due to its stabilizing effect, taxol eliminates the need for MAPs in tubulin assembly *in vitro*.<sup>163</sup>

However, in contrast to taxol, the MAP “modulates, but does not abolish, the dynamic behavior of microtubules.”<sup>164</sup> Possibly this derives from the fact that whereas regulated phosphorylation deactivates the MAPs, only concentration and binding affinity limit taxol.

### **Taxol-induced stability alters microtubule behavior**

In high concentrations, taxol increases microtubule polymerization, generating microtubule bundles.<sup>165</sup> In low concentrations (10nM), taxol decreases microtubule dynamics.<sup>166</sup> Both of these interfere with microtubule function with respect to mitosis.

In 1979, Schiff et al discovered that taxol induced tubulin polymerization *in vitro*.<sup>167</sup> The following year, these results were confirmed *in vivo*. In the cell, a drug with this mode of action causes the disruption of microtubule behavior, which in turn interferes with mitosis. Cells treated with taxol are blocked at either late G2 or at the M phase.<sup>168</sup>

Subsequent studies following up on this initial observation clarified the parameters of taxol-

---

<sup>iv</sup> The high number of negative, or acidic, amino acids prevented the placement of some of the C terminal amino acids– the last 10 of    and the last 18 of    – in the 3.7    structural model of tubulin (Nogales 1999b).

induced tubulin polymerization *in vitro* with respect to decreased need for microtubule-associated proteins (MAPs) and exogenous GTP, inhibition of assembly by microtubule destabilizing agents, and resistance to depolymerization by cold, CaCl<sub>2</sub>, and destabilizing agents. The overall picture was one of increased stability in taxol-treated microtubules. The following conditions were noted:

*In vitro*, taxol enhances polymerization,<sup>169</sup> stabilizes steady-state behavior<sup>170</sup> and confers resistance against depolymerization.<sup>171</sup> It also increases the reaction rate and raised the number of nucleations that occurred.<sup>172</sup>

*Increased polymerization.*

- In the presence of taxol, approximately 3.8 times more microtubules formed relative to the amount formed in its absence. The polymers, however, were shorter.<sup>173</sup>

- Maximum effective taxol to tubulin ratio is ~1:1.<sup>174,175</sup> This occurs at 5 M taxol concentration.<sup>176</sup>

- Upon addition of taxol, polymerization occurred until assembly again reached steady state (taxol concentration 5 M, 30 minute time frame).<sup>177</sup>

- When added to microtubules at steady state, taxol induces polymerization.<sup>178</sup> Notably, at equal concentrations of taxol (5 M) the amount of microtubule mass present equaled that of microtubules assembled in the presence of taxol.<sup>179</sup>

- Taxol can induce polymerization even in the absence of MAPs, which are normally required for assembly.<sup>180</sup> According to Kumar, the differences between taxol- and MAPs-induced assembly are: taxol does not require GTP, CaCl<sub>2</sub> does not inhibit assembly with taxol, free tubulin exchange (visualized with tritium labeled GTP) is slower in taxol, and taxol confers assembled microtubules with resistance to depolymerization by cold, CaCl<sub>2</sub>, and podophyllotoxin.<sup>181</sup> However, in contrast,

Hamel et al found that without MAPs, taxol requires both exogenous GTP and warm temperature (37°C) for its action and the resulting polymers do not have cold resistance (they exhibit slow cold reversibility), whereas in the presence of MAPs, only one or the other of GTP and warm temperature is required by taxol for polymerization and polymers assembled with GTP are cold resistant.<sup>182</sup> This differed from Schiff et al (1979) who found cold resistance in non-MAP taxol-induced polymers as well.<sup>183</sup>

- GTP, normally necessary for tubulin polymerization (for reasons explained above), is not always a prerequisite in the presence of taxol.<sup>184</sup> This relates to taxol's ability to stabilize GDP-bound tubulin, because normally, these dimers would dissociate and exchange their nucleotide for GTP in order to re-associate. Even without GTP, in the presence of MAPs, taxol formed cold resistant and CaCl<sub>2</sub> resistant microtubules.<sup>185</sup> Taxol, in fact, is "the only known ligand that can induce microtubule polymerization in the absence of -phosphate."<sup>186</sup>

- In terms of inhibiting polymerization, the microtubule destabilizers podophyllotoxin, colchicine and nocodazole interfere with assembly whereas CaCl<sub>2</sub> does not.<sup>187</sup> However, once assembled, taxol microtubules become resistant to podophyllotoxin.<sup>188</sup>

#### *Steady state.*

- Setting the stage for later studies on microtubule dynamics, the effects of taxol on treadmilling were analyzed. Since GTP is involved in polymerization, tritium labeled GTP facilitated the comparison of GTP uptake between taxol and non-taxol assemblies. Five times less uptake occurred in taxol microtubules relative to MAP microtubules once assembled, indicating a more stable steady state.<sup>189</sup>

#### *Resistance to depolymerization once assembled.*

•Microtubules induced by taxol are resistant to depolymerization by  $\text{CaCl}_2$  and— in the presence of MAPs— by cold, both of which normally disassemble microtubules.<sup>190,191</sup> Absence of GTP still allowed for stability against  $\text{CaCl}_2$ .<sup>192</sup> In addition, in contrast to non-taxol assembled polymers, taxol-assembled microtubules become resistant to the microtubule destabilizing podophyllotoxin.<sup>193</sup>

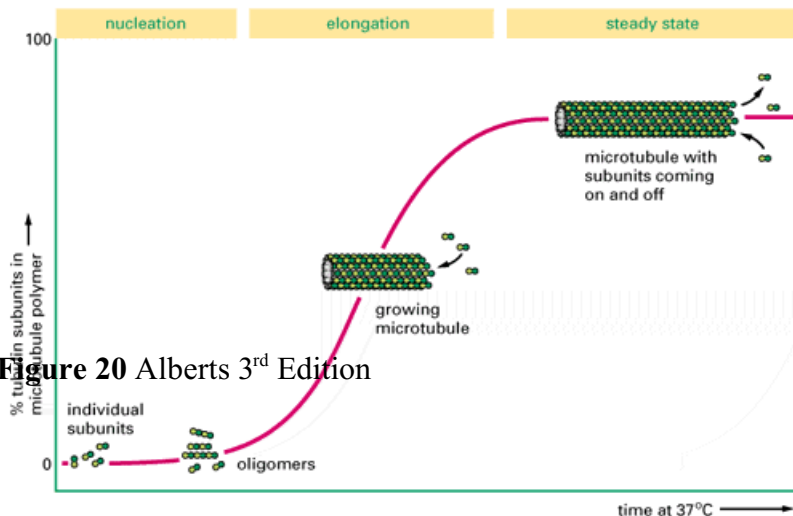
*Increased assembly rate.*

Microtubules undergo three stages of assembly: nucleation, growth, and steady state. The growth curve includes a lag time due to nucleation (see figure 20).<sup>194,195</sup> Independent of the concentration at which it is applied, taxol shortens the lag time *in vitro*.<sup>196</sup> It does so even in the absence of GTP.<sup>197</sup> It also generates new nucleations *in vitro*— the combination of tubulin, nucleation seeds and taxol (20  $\mu\text{M}$ ) generated more microtubules than did tubulin and the seeds alone, not accounted for by a difference in microtubule length.<sup>198</sup>

*Decreased critical concentration.*

The addition of subunits to polymers is concentration dependant, but this is not the case for dissociation.<sup>199</sup> Critical concentration, defined as the concentration at which the rate of addition equals that of dissociation, therefore is reached when the available free tubulin subunits “get used up.”<sup>200</sup> Since, as mentioned, the

GDP form has the lower affinity level and GTP tubulin the higher one, critical concentration depends upon the rate constant of GDP





tubulin leaving relative to the rate constant of GTP tubulin adding on.<sup>201</sup> Taxol decreases the critical concentration of tubulin normally required for polymerization to occur. In one experiment, the critical concentration of taxol-assembled microtubules 0.015mg/mL of tubulin, as compared 0.2 mg/mL for non-taxol microtubules.<sup>202</sup> By preventing the otherwise dissociation-inclined GDP dimers from breaking off of the polymer, the reduced dissociation rate constant shifts the equilibrium toward microtubule assembly and decreases the critical concentration.<sup>203</sup>

### In low concentrations, taxol stabilizes microtubule dynamics

Microtubules exhibit from 10 to 100 times more dynamic behavior during mitosis as compared to the level at interphase.<sup>204</sup> Although taxol in high concentrations induces tubulin polymerization, even in low concentrations—too low to induce microtubule assembly—the drug still inhibits cell

proliferation (see figure 21).<sup>205</sup> This is because at lower concentrations, taxol still interferes with the dynamic behavior that is essential to microtubule function.

This has been observed both *in vitro* and *in vivo*.<sup>206</sup> In

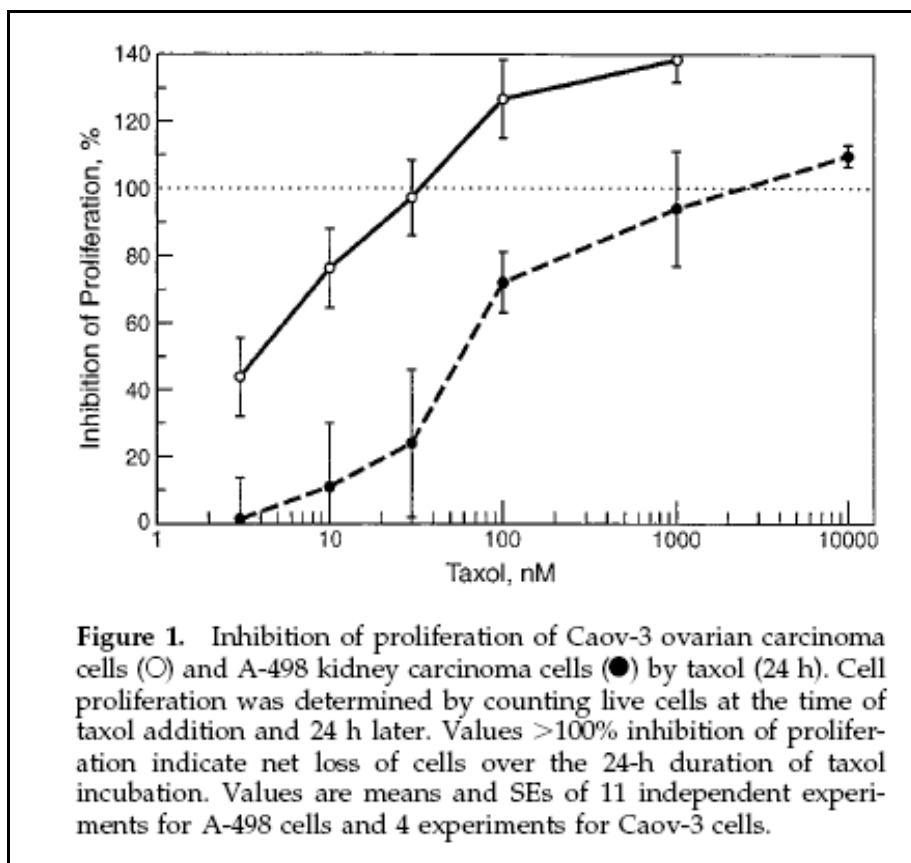


Figure 21 Yvon, 1999

normal microtubule behavior, a certain percentage of the shortening events characteristic of dynamic instability lead to depolymerization of that particular microtubule.<sup>207</sup> In vitro, at concentrations greater than 500 nM, taxol completely reverses this outcome. Though in concentrations below 500 nM, taxol does not significantly alter the amount of time spent by the microtubule in growth versus shortening versus attenuation (pause), 500 nM to 1000 nM causes a 650% increase in the amount of time spent in pause. In comparing the efficacy of various taxol/tubulin ratios on shortening, Derry et al found that a small ratio still altered dynamics.

Microtubules exhibit an even higher level of dynamics in cells than that shown *in vitro*.<sup>208</sup> In live cells, administration of taxol at concentrations that inhibit cell proliferation (but too low to induce polymerization) decreased the growth and shrinkage rates characteristic of microtubule



Fig. 1. Dynamic behavior of microtubules in living A549 cells. Arrows indicate three microtubules that undergo shortening events. Time is indicated as min:s.

**Figure 22** “Dynamic behavior of microtubules in living A549 [lung cancer] cells. Arrows indicate three microtubules that undergo shortening events. Time is indicated as min:s.” [Gonclaves, A et al. (2001). Resistance to Taxol in Lung Cancer Cells Associated with Increased Microtubule Dynamics. *Proc. Natl. Acad. Sci.* 98, 11737-11741.]

dynamics.<sup>209</sup> Shortening rate decreased by 31% in caov-3 ovarian cancer cells and by 26% in A-498 kidney carcinoma cells, while growth rate decreased by 24% in caov-3 cells and by 18% in A-498

cells (to offset the fact that taxol acts with different strength on different cancer cell types, two cell lines were studied).<sup>210</sup>

Overall dynamicity—measured as the sum of growth and shrinkage lengths divided by the life-span of the microtubule—decreased by 31% in caov-3 and 63% in A-498 cells. Decreased dynamics interfered with the mitotic spindle. Mitotic cells showed abnormal spindle, either multipolar with disorganized chromosomes or the normal bipolar but with “lagging” chromosomes<sup>211</sup> not in their proper place. Mitotic cells appearing in higher than normal proportions indicated blocking of mitosis.<sup>212</sup> For example, certain concentrations of taxol

completely blocked caov-3 cells between metaphase and anaphase. These observations indicate that low concentrations of taxol are enough not only to disrupt dynamics but to hinder the mitotic spindle and halt mitosis.

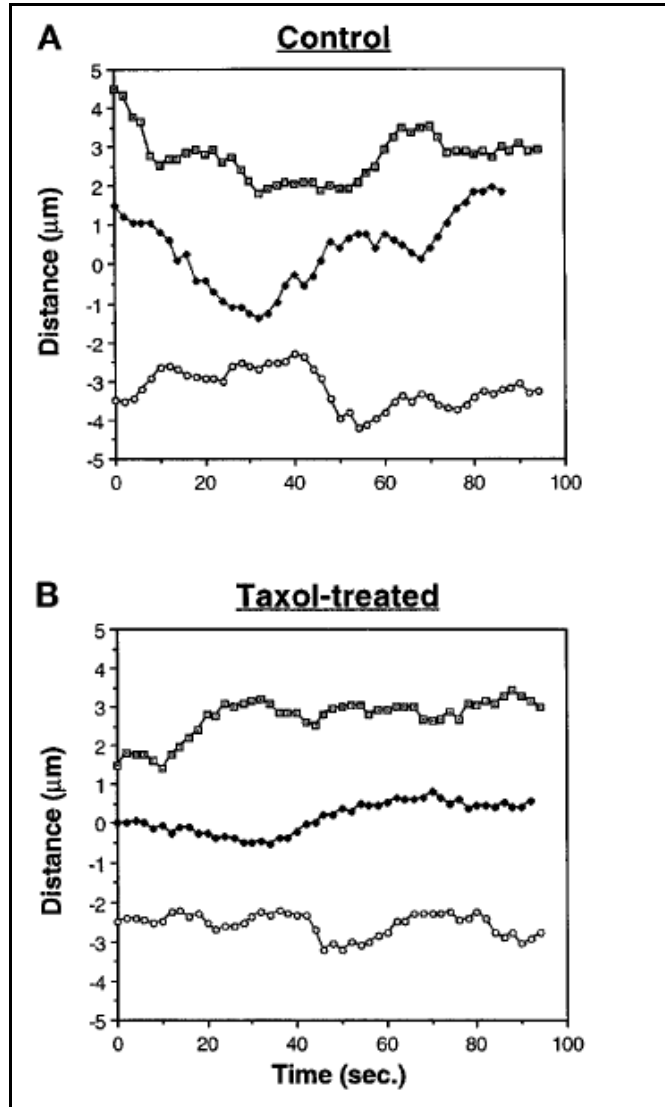


**Figure 23** Effect of taxol on Caov-3 ovarian cancer cells. Microtubules in B) are more static than they are in A). (Yvon 1999).

completely blocked caov-3 cells between

metaphase and anaphase. These observations indicate that low concentrations of taxol are enough not only to disrupt dynamics but to hinder the mitotic spindle and halt mitosis.

### Dysfunctional spindle leads to aberrant mitosis and/or apoptosis

Once taxol binds to the microtubules and disrupts their behavior, how does the cell respond?

Taxol is “more cytotoxic in G2/M than in S phase.”<sup>213</sup> For a cell that is undergoing mitosis, malfunctioning of the spindle fibers could have catastrophic effects, blocking mitosis and driving

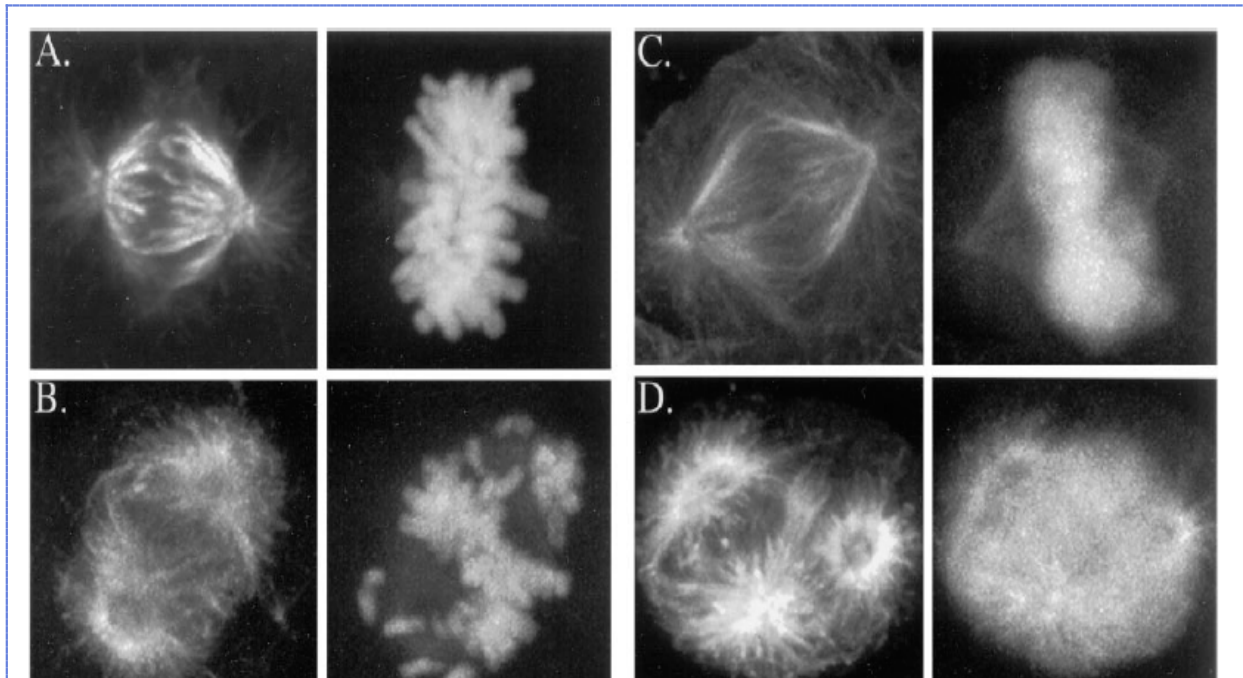


**Figure 24** Effect of taxol on mitotic spindle and chromosome arrangement in two cancer cell lines: A and B are kidney cells (A-498) and C and D are ovarian cells (Caov-3). A and C show the mitotic spindle without taxol, and images to the right depict chromosomes. Bottom row shows the effects of taxol: chromosomal arrangement altered in both, multipolar spindle in D.

the cell into apoptosis (programmed cell death). Or, mitosis might still occur but this mitosis could be abnormal and likewise lead to apoptosis. Apoptosis has been observed in tumor cells that received taxol.<sup>214</sup>

As the cell progresses through the four stages of its cycle– G1, S, G2, M– it maintains a checkpoint system to insure that the proper conditions for progression to the next stage are in

place.<sup>215</sup> This checkpoint system consists of a G1 check to determine whether DNA replication should proceed, a G2 check to ascertain whether DNA has been properly replicated for entry into mitosis, and a metaphase checkpoint to ensure that all chromosomes are attached to kinetochores before anaphase occurs.<sup>v.216</sup> Taxol, through its disruption of the mitotic spindle, can bring about incomplete attachment of microtubules to kinetochores, and thus can prevent mitosis from continuing on to anaphase for failure to pass the metaphase checkpoint.<sup>217</sup> In terms of how the metaphase checkpoint works: usually, the transition from metaphase to anaphase takes place when the anaphase-promoting complex (APC) initiates chromosome separation.<sup>218</sup> However, the binding of certain proteins to unattached chromosomes is the checkpoint signal that halts this process.<sup>219</sup> It is possible that in taxol-treated cells, failure to pass through this checkpoint is the cause of apoptosis. As an example of checkpoint status in cancer cells, Masuda et al found deficiency in approximately 40% of the human lung cancer cell lines they studied.<sup>220</sup> Checkpoint impaired cells, indeed, show increased resistance to taxol, because although the drug can disrupt kinetochore attachment, the checkpoint has lost its capacity to respond to the problem.

Masuda et al examined this system by comparing the proportion of apoptosis occurring in response to anti-microtubule drugs in checkpoint intact cancer cells compared to that in checkpoint impaired cancer cells.<sup>221</sup> (Their method of determining which cell lines were checkpoint inhibited was to test their response to nocadazole, an anti mitotic drug itself, to see what number of cells in each became blocked at prometaphase and to confirm the absence of mitotic phase-specific proteins in cells that passed this point).<sup>222</sup> The study, however, used taxotere rather than taxol. In response

---

<sup>v</sup> Checkpoints also respond to environmental cues to ensure that external conditions are favorable for cell division.

to taxotere, only 25% of a checkpoint inhibited cell line underwent apoptosis, as compared to the 53% of a checkpoint capable cell line, and tests on thirteen additional cell lines confirmed this trend<sup>vi</sup>.<sup>223</sup> It is a reasonable assumption that even in a situation in which the microtubules have become disturbed by anti-microtubule drugs, if the system fails to respond to the disruption, mitosis could proceed in spite of it.

However, as reported elsewhere, mitosis that does occur in taxol treated cells could still be of an aberrant nature. Cancer cells (A549 line) that received low concentrations of taxol avoided mitotic block but underwent a mitosis characterized by multipolar spindles, which led to aneuploid daughter cells.<sup>224</sup> Not always does the checkpoint need to be inactive for cells to bypass it in spite of compromised microtubules. Even with multipolar spindles, as long as the chromosomes are lined up, mitosis can proceed.<sup>225</sup> However, the aneuploidy induced by the atypical polarity ultimately still drives cells into apoptosis, usually as a consequence of lethal genetic imbalance— the chromosomal distribution was such that not all the genes necessary for survival are present.<sup>226</sup>

In contrast to the microtubule stabilizing drugs, the destabilizers do not induce aberrant mitosis, even though both stabilize microtubule dynamics.<sup>227</sup>

The outcome of the surviving cells in the Mesuda et al study is not described, but would be of interest because another drug that was used was nicodazole, a destabilizing agent.

Cells treated with low concentrations of taxol showed an increase in the number of multinucleate cells at interphase (70.7% as compared to 3% in A-498, 29.7% as compared to 1.4% in caov-3) manifesting a number of large or “lobulated” nuclei or many small nuclei.<sup>228</sup> Based upon

---

<sup>vi</sup> Variations in p53 tumor suppressor was eliminated as a variable because all cells were p53 wild type. Specificity to anti-microtubule drugs was proven by failure of DNA disrupting drug cis-platin to induce such a distinction.

these observations, it has been suggested that taxol-treated cells that can no longer complete mitosis revert to a multinucleate interphase-like state.

### **Is taxol-induced Bcl2 phosphorylation responsible for apoptosis?**

Bcl2 and related proteins normally keep apoptosis in check. However, phosphorylation inactivates bcl2.<sup>229</sup> Bcl2 phosphorylation has been correlated with taxol.

Not all agree that the bcl2 phosphorylation that occurs in response to taxol is responsible for apoptosis. Bcl2 appears also to be involved in mitosis. One study of nocodazole, a microtubule destabilizer, showed that checkpoint proficient cells had high amounts of phosphorylated bcl2 whereas impaired cells had low amounts that remained in proportion with the number of mitotic cells.<sup>230</sup>

Moreover, the pathway through which taxol induces the phosphorylation has also not been definitively determined (Abal 2003).

### **Tumor necrosis factor**

An additional aspect has been implicated in taxol's activity, namely the release of tumor necrosis factor type (TNF- ) by macrophages that surround the tumor.<sup>231</sup> This was analyzed by Lanni et al. in an effort to account for the fact that while taxol was effective against tumors (preclinical study) without differentiating between p53 tumor suppressor wild type or mutant, when taxol was applied to cells in the lab, it had more activity against p53 wild type. This led to the conclusion that a tumor dependant factor, present only with tumors but absent from separate cells, is responsible for this distinction.<sup>232</sup> For this reason, TNF- , released from tumor associated macrophages, was studied. Mouse macrophages treated with taxol seemed to release this compound, and it was shown to induce apoptosis even in p53 negative cells.<sup>233</sup> Human macrophages do not

release TNF- $\alpha$  in response to taxol alone but do so with the addition of LPS (lipopolysaccharide).<sup>234</sup> This raises the possibility that taxol can trigger TNF- $\alpha$  release from macrophages.<sup>235</sup> However, Lanni et al. conclude that further research on the effect of taxol on immune system response is needed.

## **Resistance**

Although cells initially respond to cancer treatment, in some cases, resistance may develop. Though the method is not fully understood, a number of processes have been implicated in taxol resistance. For instance, cells with abnormally high levels of dynamics will not be hindered by taxol. In fact, some of these cells become dependant upon taxol. Additionally, mutations in both the beta and alpha monomers can prevent taxol from binding.<sup>236</sup> For example, one resistant cell line showed a mutation at 270. The map of secondary structure by Lowe et al shows this to be right before the start of the M-loop, the main site of taxol interaction.<sup>237</sup> The mutation at 279 replaced phenylalanine with valine, and loss of the phenyl group from phenylalanine could alter the way in which taxol binds to tubulin at that site.<sup>238</sup> In further support of the contribution of tubulin mutations to resistance, an initial study found  $\beta$ -tubulin mutations in DNA samples of a noteworthy amount of patients with a particular type of lung cancer.<sup>239</sup> These results are being confirmed by additional studies.<sup>240</sup> As an additional factor, the p-glycoprotein drug efflux pump confers multi-drug resistance against hydrophobic anti-tumor drugs such as taxol.<sup>241</sup> Overexpression of the p-glycoprotein multi-drug transporter pumps taxol out before it has a chance to bind. Additionally, taxol is involved in other pathways that lead to apoptosis. For example, taxol has been shown possibly to phosphorylate, thereby inactivating, the proteins bcl2 and bcl-xl, both of which normally restrain apoptosis. However, if something occurs to prevent taxol from having its normal effect on these pathways,



resistance could develop.<sup>242</sup>

### **Other anti-microtubule drugs include stabilizers and destabilizers**

Two classes of anti-microtubule agents exist. In addition to taxol, those that stabilize include taxol, epithilone B, discodermolide (Chen 2003) and epithilone A and eleutherobin (Ojima, 1999). Destabilizers include vinblastine, colchicine and nocodazole (Chen 2003). Both stabilizers (taxol) and destabilizers (vinblastine) decrease dynamic behavior at low concentrations (Chen 2003). However, whereas taxol preferentially binds to the assembled microtubule, colchicine binds to individual tubulin (Rao 1995). It would therefore seem as though stabilization prevents subunits from leaving while destabilization prevents them from adding on, ultimately with the same effect on dynamics. By way of speculation, it perhaps it would be possible to view the slowed dynamics as a macro version of a pause and polymerization upon stabilization (high enough concentrations) would be a macro rescue while depolymerization upon destabilization would be akin to a catastrophe.

### **Conclusion**

By stabilizing the M-loop, taxol disturbs the microtubules. Dysfunctional microtubules then bring about abnormal mitosis or prevent it from occurring altogether. Cells in late growth or in mitosis seem to experience a greater response to taxol, possibly to due the increased mobility required during these stages as the cytoskeleton reassembles into the spindle and as the spindle organizes the chromosomes at the mitotic plate. Much still remains to be learned about taxol. For example, what causes resistance. Can structural and kinetic views of its binding conclusively be reconciled. Is bcl2 phosphorylation in fact a significant factor

in its activity. Beyond the scope of this paper, how toxic is it to non-cancerous cells. Involvement of the p53 tumor suppressor is being studied (Lanni 1997). As cancer research continues, presumably more will be learned about taxol, which will lead to more successful treatments.

1. Horowitz, SB (1994). How to Make Taxol from Scratch. *Nature*. 367, 593-4.
2. Edwards, N. Molecule of the Month: Taxol. July 12, 1996. School of Chemistry, University of Bristol. August 20, 2003. <<http://www.bris.ac.uk.Depts/Chemistry/MOTM/taxol/taxol.htm>
3. Ibid.
4. Raven, Peter, Ray Evert and Susan Eichhorn. Biology of Plants. New York: W.H. Freedman & Company/Worth Publishers, 1999.
5. Stierle, A et al. (1993). Taxol and Taxane Production by *Toxomyces andreanae*, an Endophytic Fungus of Pacific Yew. *Science*. 260, 214-216.
6. Ibid.
7. Horowitz SB, 1994.
8. Lavelle, F (1995). Preclinical Evaluation of Docetaxel. *Semin. Oncol.* 2 (Suppl. 4), abstract p3.
9. Andreu JM et al. (1994). Solution Structure of Taxotere-Induced Microtubules to 3-nm Resolution. *Journal of Biological Chemistry*. 269, 31785-31792.
10. Stierle, A et al., 1993.
11. "From a Fungus, a Cancer Cure Seems to Grow" *Newsweek*. April 19, 1993.
12. Edwards, N. Molecule of the Month: Taxol. July 12, 1996. School of Chemistry, University of Bristol. August 20, 2003. <<http://www.bris.ac.uk.Depts/Chemistry/MOTM/taxol/taxol.htm>
13. Abal, M et al. (2001). Centrosome and Spindle Pole Microtubules Are Main Targets of a Fluorescent Taxoid Inducing Cell Death. *Cell Motility and the Cytoskeleton*. 49, 1-15.
14. Horowitz SB, 1994
15. Rao, S et al. (1995). Characterization of the Taxol Binding Site on the Microtubule. *The Journal of Biological Chemistry*. 270, 20235-20238.
16. Ojima, I et al. (1999) A Common Pharmacophore for Cytotoxic Natural Products that Stabilize Microtubules. *Proc. Natl. Acad. Sci. USA*. 96, 4256-4261.
17. Snyder, JP et al. (2001). The Binding Conformation of Taxol in beta-Tubulin: A Model Based on Electron Crystallographic Density. *Proc. Natl. Acad. Sci., USA*. 98, 5312-5316.
18. Abal M et al., 2001.
19. Ibid.
20. Andreu JM et al, 1994

21. Snyder JP et al, 2001. Bruice, PY. (2001) Organic Chemistry. New Jersey: Prentice Hall.
22. Bruice PY, 2001
23. Snyder, JP et al. (2001). The Binding Conformation of Taxol in  $\alpha$ -tubulin: A Model Based on Electron Crystallographic Density. *Proc. Natl. Acad. Sci. USA*. 98, 5312-5316.
24. Ibid.
25. Ibid.
26. Taiz, Lincoln and Eduardo Zeiger. Plant Physiology, 3<sup>rd</sup> Ed. Massachusetts: Sinauer Associates Inc., 2002.
27. Ibid.
28. Stierle, A et al. (1993). Taxol and Taxane Production by *Toxomyces andreanae*, an Endophytic Fungus of Pacific Yew. *Science*. 260, 214-216.
29. Ibid.
30. Schiff, PB et al. (1979) Promotion of Microtubule Assembly in vitro by Taxol. *Nature*. 277, 665-667.
31. Downing, K and E Nogales (1998). New Insights into Microtubule Structure and Function from the Atomic Model of Tubulin.
32. Meurer-Grob
33. Downing, K and E Nogales (1998). New Insights into Microtubule Structure and Function from the Atomic Model of Tubulin.
34. Nogales et al. (1998). Structure of the  $\alpha$ -Tubulin Dimer by Electron Crystallography. *Nature*. 391,199-203.
35. Ibid.
36. Ibid.
37. Lowe, J et al. (2001). Refined Structure of  $\alpha$ /beta-Tubulin at 3.5 Angstrom Resolution. *Journal Molecular Biology*. 313, 1045-1057.
38. Ibid.
39. Keskin, O et al. (2002). Relating Molecular Flexibility to Function: A Case Study of Tubulin. *Biophysics Journal*. 83, 663-680.
40. Lowe J 2001, Keskin O 2002, Nogales E, 1998.
41. Nogales E et al. (1999a). High Resolution Model of the Microtubule. *Cell*. 96, 79-88.

42. Keskin, O et al. (2002). Relating Molecular Flexibility to Function: A Case Study of Tubulin. *Biophysics Journal*. 83, 663-680.
43. Keskin, O et al. (2002). Relating Molecular Flexibility to Function: A Case Study of Tubulin. *Biophysics Journal*. 83, 663-680.
44. Ibid.
45. Ibid.
46. Ibid.
47. Ibid.
48. Rao O et al. (1999). Characterization of the Taxol Binding Site on the Microtubule. *Journal Biological Chemistry*. 274, 37990-37994.
49. Nogales E, 1998.
50. Snyder
51. Snyder
52. Snyder
53. Snyder
54. Snyder
55. Lowe
56. Lowe
57. Snyder
58. Lowe
59. Lowe
60. Snyder
61. Lowe
62. Snyder
63. Snyder
64. Snyder
65. Snyder
66. Snyder

67. Snyder
68. Lowe
69. Snyder
70. Nogales E, 1999a
71. Snyder
72. Keskin
73. Keskin
74. Keskin
75. Keskin
76. Keskin
77. Keskin
78. Keskin
79. Alberts, Fourth Edition.
80. Alberts
81. Alberts
82. Meurer-Grob, P.(2001). Microtubule Structure at Improved Resolution. *Biochemistry*. 40, 8000-8008.
83. Ross JL and DK Fygenson. (2003). Mobility of Taxol in Microtubule Bundles. *Biophys. Journal*. 84, 3959-3967.
84. Meurer-Grob
85. Meurer-Grob
86. Meurer-Grob
87. Ross JL, 2003.
88. Nogales, E et al., 1999a
89. Ibid.
90. Alberts
91. Alberts

92. Nogales
93. Lowe
94. Lowe
95. Nogales, E. 1999a
96. Nogales E, 1999a
97. Keskin
98. Nogales E, 1999a
99. Nogales E, 1999a
100. Meurer-Grob
101. Meurer-Grob
102. Keskin
103. Keskin
104. Nogales E, 1999a
105. Lowe
106. Meurer-Grob
107. Andreu 1998 Changes in #
108. Andreu JM et al (1994). Solution Structure of Taxotere-induced Microtubules to 3-nm Resolution. *The Journal of Biological Chemistry*. 269, 31785-31792.
109. Ibid.
110. Meurer-Grob
111. Meurer-Grob
112. Meurer-Grob
113. Nogales, E 1999a.
114. Diaz, JF et al. (2000). Molecular Recognition of Taxol by Microtubules. *The Journal of Biological Chemistry*. 275, 26265-26276.
115. Ibid.
116. Ibid.

117. Ibid.
118. Andreu 1994
119. Andreu 1994
120. Ross JL et al. (2003). Mobility of Taxol in Microtubule Bundles. *Biophysical Journal*. 84, 3959-3967.
121. Ghosh
122. Alberts
123. Hamel, E et al. (1981). Interactions of Tubulin, Microtubule-associated Proteins, and Guanine Nucleotides in Tubulin Polymerization. *The Journal of Biological Chemistry*. 256, 11887-11894.
124. Hamel, E et al., 1981.
125. Downing KH and E Nogales. (1998). New Insights Into Microtubule Structure and Function from the Atomic Model of Tubulin. *Eur. Biophys. Journal*. 27, 431-416.
126. Lowe
127. Keskin
128. Nogales, E. (1999b) A Structural View of Microtubule Dynamics. *Cell and Molecular Life Sciences*. 56, 133-142.
129. Nogales, E. 1999a.
130. Lowe
131. Lowe
132. Lowe
133. Meurer-Grob
134. Nogales, 1999b.
135. Alberts.
136. Alberts
137. Downing, K 1998
138. Downing, K 1998
139. Diaz, JF et al (1998). Changes in Protofilament Number Induced by Taxol Binding to an Easily Accessible Site. *Journal of Biological Chemistry*. 273, 33803-33810.



140. Meurer-Grob
141. Nogales, E. 1999a.
142. Meurer-Grob
143. Alberts
144. Nogales 1999b
145. Nogales 1999b
146. Keskin
147. Schiff 1979.
148. Yvon
149. Alberts
150. Alberts
151. Nogales 1999b
152. Schiff, PB et al. (1979). Promotion of Microtubule Assembly in vitro by Taxol. *Nature*. 277, 665-667.
153. Hirokawa, N. (1994). Microtubule Organization and Dynamics Dependent on Microtubule-associated Proteins. *Current Opinion in Cell Biology*. 6, 74-81.
154. Drewes, G. et al (1998). MAPs, MARKs and Microtubule Dynamics. *TIBS*. August 23, 1998, 307-311.
155. Hirokawa, N. 1994
156. Drewes, G. 1998.
157. Drewes, G. 1998.
158. Hirokawa, N. 1994.
159. Hirokawa, N. 1994.
160. Hirokawa, N. 1994.
161. Drewes, G. 1998.
162. Drewes, G. 1998.
163. Schiff, PB 1979.
164. Hirokawa, N. 1994

165. Rao, 1999
166. Rao, 1999
167. Schiff 1979
168. Schiff 1979
169. Schiff 1979
170. Kumar, N. (1981) Taxol Induced Polymerization of Tubulin: Mechanism of Action. *Journal of Biological Chemistry*. 256, 10435-10441.
171. Kumar
172. Schiff PB and SB Horowitz. (1981). Taxol Assembles Tubulin in the Absence of Exogenous Guanosine 5'-Triphosphate or Microtubule-Associated Proteins. *Biochemistry*. 20, 3247-3252.
173. Schiff 1979
174. Schiff 1979
175. Kumar
176. Derry
177. Schiff PB and SB Horowitz. (1981). Taxol Assembles Tubulin in the Absence of Exogenous Guanosine 5'-Triphosphate or Microtubule-Associated Proteins. *Biochemistry*. 20, 3247-3252.
178. Schiff 1981
179. Schiff 1981
180. Kumar, N. (1981) Taxol Induced Polymerization of Tubulin: Mechanism of Action. *Journal of Biological Chemistry*. 256, 10435-10441.
181. Kumar
182. Hamel
183. Hamel et al.
184. Kumar
185. Schiff 1981
186. Nogales E et al. (1995) Structure of Tubulin at 6.5 Angstrom and the Location of the Taxol Binding Site. *Nature*. 375, 424-427.

187. Kumar
188. Kumar
189. Kumar
190. Schiff 1979.
191. Kumar
192. Schiff, PB and SB Horowitz. (1981). Taxol Assembles Tubulin in the Absence of Exogenous Guanosine 5'-Triphosphate or Microtubule-Associated Proteins. *Biochemistry*. 20, 3247-3252.
193. Kumar
194. Schiff 1981
195. Kumar
196. Schiff 1979
197. Schiff, 1981
198. Schiff 1981
199. Alberts
200. Alberts
201. Alberts
202. Schiff 1981
203. Schiff 1979
204. Yvon, AMC et al. (1999). Taxol Suppresses Dynamics of Individual Microtubules in Living Tumor Cells. *Molecular Biology of the Cell*. 10, 947-959.
205. Yvon
206. Yvon, 1999.  
Derry, WB et al. (1995). Substoichiometric Binding of Taxol Suppresses Microtubule Dynamics. *Biochemistry*. 34, 2203-2211.
207. Derry 1995
208. Nogales, E. Structural View...
209. Yvon
210. Yvon

211. Yvon
212. Yvon
213.  
Paoletti, A et al. (1997). Pulse Treatment of Interphasic HeLa Cells with Nanomolar Doses of Docetaxel Affects Centrosome Organization and Leads to Catastrophic Exit of Mitosis. *Journal of Cell Science*. 110, 2403-2415.
214. Panvichian, R et al. Signaling Network of Paclitaxel-induced Apoptosis in the LNCaP Prostate Cancer Cell Line. *Urology*. 54, 746-752.
215. Alberts
216. Alberts
217. Abal 2001.
218. Alberts
219. Alberts
220. Masuda, A et al. (2003). Association Between Mitotic Spindle Checkpoint Impairment and Susceptibility to the Induction of Apoptosis by Anti-Microtubule Agents in Human Lung Cancers. *American Journal of Pathology*. 163, 1109-1116.
221. Masuda
222. Masuda
223. Masuda
224. Chen, J and SB (2002). Horowitz. Differential Mitotic Responses to Microtubule-stabilizing and -destabilizing Drugs. *Cancer Research*. 62, 1935-1938.
225. Chen
226. Chen
227. Chen
228. Yvon
229. Panvichian, R et al. Signaling Network of Paclitaxel-induced Apoptosis in the LNCaP Prostate Cancer Cell Line. *Urology*. 54, 746-752.
230. Masuda
231. Lanni, JS et al. (1997) p53-independent Apoptosis Induced by Paclitaxel through an Indirect Mechanism. *Proc. Natl. Acad. Sci, USA*. 94, 9679-9683.

232. Lanni
233. Lanni
234. Lanni
235. Lanni
236. Orr, GA et al. (2003) Mechanisms of Taxol Resistance Related to Microtubules. *Oncogene*. 22, 7280-7295.
237. Lowe 2001.
238. Orr
239. Orr
240. Orr
241. Greenberger, LM. (1991) Domain Mapping of the Photoaffinity Drug-binding Sites in P-glycoprotein Encoded by Mouse *mdr1b*\*. *Journal of Biological Chemistry*. 266, 20744-20751.
242. Oncogenic Resistance to Growth-limiting Conditions. (2002). *Nature Reviews Cancer*. 2, 221-224 (figure 3).